

EFFECT OF HYDROFLUORIC ACID ETCHING FOLLOWED BY UNFILLED
RESIN APPLICATION ON THE BIAXIAL FLEXURAL STRENGTH OF
A GLASS-BASED CERAMIC

by

Sumana Posritong

Submitted to the Graduate Faculty of the School of
Dentistry in partial fulfillment of the requirements
for the degree of Master of Science in Dentistry,
Indiana University School of Dentistry, 2012.

This thesis accepted by the faculty of the Department of Prosthodontics, Indiana University School of Dentistry, in partial fulfillment of the requirements for the degree of Master of Science in Dentistry.

David T. Brown

Suteera Hovijitra

T.M. Gabriel Chu

Marco C. Bottino

Chair of the Research Committee

John A. Levon

Program Director

Date _____

DEDICATION

This thesis is dedicated to my beloved parents, Dr. Pollasanha and Noparat Posritong,
who made all of this possible, for their endless encourage and patience.

ACKNOWLEDGMENTS

There are many people who I wish to thank for their contribution and support. The completion of this thesis would not be possible without their assistance and support.

First of all, I would like to acknowledge the Royal Thai Government Scholarship who fully sponsored my MSD study at Indiana University School of Dentistry.

I would like to express my sincere gratitude to my thesis mentor; Dr. Marco C. Bottino, for all of his valuable help, advice, guidance, dedication, encouragement and patience in reading the drafts of my proposal and thesis. I feel extremely fortunate to have had an opportunity to work with such a dedicated individual.

I am very grateful to Dr. John A. Levon; my program director, for giving me an opportunity to study in graduate prosthodontics program, supervision and knowledgeable throughout my postgraduate study. Moreover, I would like to thank and sincerely appreciate to all of committee members; Dr. David T. Brown, Dr. Suteera Hovijitra and Dr. T.M. Gabriel Chu. Particularly to Dr. Suteera Hovijitra for her unlimited support during the years I have been in the US.

I also appreciate the assistance of Dr. Alexandre Borges, Meaghan MacPherson and Jeana Arango for their assistance that allowed me to complete my thesis.

Furthermore, this thesis would not have been possible without the support from Delta Dental Foundation and Ivoclar-Vivadent.

Most importantly, I wish to express my heartfelt gratitude to my beloved family especially my parents and my sister for all unconditional love, strong moral support and continuous encouragement. I could not have done this study without all of them.

TABLE OF CONTENTS

Introduction.....	1
Review of Literature.....	5
Materials and Methods.....	15
Results.....	21
Figures and Tables.....	26
Discussion.....	59
Summary and Conclusions.....	65
References.....	67
Abstract.....	74
Curriculum Vitae	

LIST OF ILLUSTRATIONS

TABLE I Dental ceramics classification.....	27
TABLE II Description of the experimental groups.....	28
TABLE III Firing cycle of IPS e.max ZirPress according to manufacturer's recommendation	29
TABLE IV Means (MPa) \pm SD, \pm SE and range of biaxial flexural strength of experimental groups	30
TABLE V Flexural strength means (δ), and statistical parameters (δn_0 and m) obtained from the Weibull Distribution of the initial mechanical strength.....	31
FIGURE 1 Demonstration of measurement of the wax pattern.....	32
FIGURE 2 Macrophotograph of sprued wax patterns.....	33
FIGURE 3 Illustration of wax patterns attached to the sprue former	33
FIGURE 4 Macrophotographs of a wax pattern mold ready for investing.....	34
FIGURE 5 IPS PressVest Speed powder and liquid (Ivoclar-Vivadent).....	35
FIGURE 6 IPS e.max ZirPress ingots (Ivoclar-Vivadent).....	35
FIGURE 7 Furnace Programat EP 5000 (Ivoclar-Vivadent)	36
FIGURE 8 Pressed investment rings.....	36
FIGURE 9 Representative of IPS e.max ZirPress (Ivoclar-Vivadent) polished ceramic specimens.....	37
FIGURE 10 Macrophotographs of IPS ceramic etching gel, Monobond Plus, and Heliobond (Ivoclar-Vivadent).....	37
FIGURE 11 Schematic representation of the etching and surface treatment procedures.....	38
FIGURE 12 Illustration of specimens preparation for SEM.....	39

FIGURE 13 A JEOL SEM (JSM – 6390) used for surface micro-morphological evaluation	39
FIGURE 14 Schematic representation of a-piston-on-three-ball jig for biaxial flexural test.....	40
FIGURE 15. Illustration of a-three-ball-jig for biaxial flexural strength.....	41
FIGURE 16 A universal testing machine (MTS Sintech ReNew 1123) used for biaxial flexural test	42
FIGURE17 Illustration of ceramic specimen set up on a -three-ball jig.....	43
FIGURE 18 Illustration of ceramic specimen set up on a-three-ball jig and the position of a piston ready for loading.....	43
FIGURE 19 Illustration of ceramic specimen fracture after force loading.....	44
FIGURE 20 Representative SEM micrographs of the as-polished ceramic group (A) at $\times 500$ magnification and (B) at $\times 1500$ magnification.....	45
FIGURE 21 Representative SEM micrograph of the as-polished ceramic group at higher magnification ($\times 3500$)	45
FIGURE 22 Representative SEM micrographs of the 30 s etched ceramic group (A) at $\times 500$ magnification and (B) at $\times 1500$ magnification.....	46
FIGURE 23 Representative SEM micrograph of the 30 s etched ceramic group at higher magnification ($\times 3500$)	46
FIGURE 24 Representative SEM micrographs of the 60 s etched ceramic group (A) at $\times 500$ magnification and (B) at $\times 1500$ magnification.....	47
FIGURE 25 Representative SEM micrograph of the 60 s etched ceramic group at higher magnification ($\times 3500$)	47

FIGURE 26 Representative SEM micrographs of the 90 s etched ceramic group
 (A) at $\times 500$ magnification and (B) at $\times 1500$ magnification..... 48

FIGURE 27 Representative SEM micrograph of the 90 s etched ceramic group at
 higher magnification ($\times 3500$) 48

FIGURE 28 Representative SEM micrographs of 120 s etched ceramic group
 (A) at $\times 500$ magnification and (B) at $\times 1500$ magnification. 49

FIGURE 29 Representative SEM micrograph of 120 s etched ceramic group at
 higher magnification ($\times 3500$).. 49

FIGURE 30 Representative SEM micrographs of re-etched ceramic group
 (A) at $\times 500$ magnification and (B) at $\times 1500$ magnification. 50

FIGURE 31 Representative SEM micrograph of re-etched ceramic group at
 higher magnification ($\times 3500$)..... 50

FIGURE 32 Representative SEM micrographs of as polished ceramic with unfilled resin
 application (A) at $\times 250$ magnification and (B) at $\times 500$ magnification.. 51

FIGURE 33 Representative SEM micrographs of 30 s etched ceramic with unfilled resin
 application (A) at $\times 250$ magnification and (B) at $\times 500$ magnification..... 52

FIGURE 34 Representative SEM micrographs of 60 s etched ceramic with unfilled resin
 application (A) at $\times 500$ magnification and (B) at $\times 1500$ magnification. 53

FIGURE 35 Representative SEM micrographs of 90 s etched ceramic with unfilled resin
 application (A) at $\times 500$ magnification and (B) at $\times 1500$ magnification.. 54

FIGURE 36 Representative SEM micrographs of 120 s etched ceramic with unfilled resin
 application (A) at $\times 500$ magnification and (B) at $\times 1500$ magnification..... 55

FIGURE 37 Representative SEM micrographs of re-etched ceramic with unfilled resin application (A) at $\times 250$ magnification and (B) at $\times 500$ magnification.. 56

FIGURE 38 Flexural strength means and respective \pm SD of IPS ZirPress specimens.....57

FIGURE 39 Survival probability plotted on Weibull model of experimental groups.....58

INTRODUCTION

All-ceramic restorations have become more prevalent in recent years due to their high esthetics, which can mimic the natural teeth appearance, biocompatibility and good mechanical properties. As a consequence, numerous ceramic systems for indirect restorations ranging from veneers to multiple-unit posterior fixed dental prostheses (FDPs) as well as to dental implant restorations have been developed and used clinically in oral rehabilitation.^{1,2}

The success of all-ceramic restorations (e.g., porcelain laminated veneers/PLV, inlays, onlays and crowns) depends not only of a meticulous tooth preparation, laboratory and clinical techniques of ceramic processing and preparation, respectively, but also on the retention of these restorations to the tooth structure. To date, the retention of ceramic restorations to the tooth structure can be accomplished by establishing a reliable bond between the internal surface of the restoration and the cement. Briefly, the bond formation between the ceramic and cement is typically achieved via micro-mechanical interlocking between the once etched (e.g., hydrofluoric/HF acid, acidulated phosphate fluoride/APF) or air-abraded (e.g., aluminum oxide particles) ceramic internal surface and a resin-based cement. After etching or air-abrasion of the ceramic internal surface, the use of a silane coupling agents is often employed to promote also a chemical component by the formation of siloxane covalent bond and hydrogen bonds.³⁻⁷

A great body of literature has been published supporting the use of HF acid etching as one of the most effective methods regarding the achievement of high bond

strength values and a durable bond between glass-based ceramics and resin cements. The rationale for these high bond strength values after etching is based on the fact that HF etching amplifies the ceramic surface roughness and surface energy by means of a selective removal of the glassy-phase and crystalline structure exposure. This improves the interaction ceramic surface-resin cement.⁸⁻¹¹ As mentioned previously, the application of a silane coupling agent after ceramic etching provides for chemical bonding as well as increases the ceramic wettability, and therefore its cohesiveness to resin cements.^{5, 10} While APF etching has led to inferior bond strength results when compared to either HF or alumina particles air-abrasion, it presents a less hazardous effect than HF and has been advocated for intraoral ceramic repair.¹²⁻¹⁴ Regarding aluminum oxide air-abrasion, this technique is commonly used for cleaning off the investment from porcelain in the dental laboratory and also can be used intraorally for porcelain surface cleaning before ceramic repair. Unfortunately, according to Roulet et al.¹⁵, the air-abraded surfaces are most likely not ideal for bonding since sharp irregularities might serve as stress concentration points which could lead to fracture within the ceramic material.

Thus far, many studies have shown that distinct HF acid etching regimens tend to affect the bond strength of glass-based ceramics to resin cements.^{6, 9, 11, 16} Nonetheless, the HF acid etching effect on its mechanical properties remains uncertain and only few, contradictory studies have reported about the effect of an unfilled resin (UR) application after silane treatment on the ceramic flexural strength.¹⁷⁻²⁰ Therefore, the objectives of this study were threefold: (1) to investigate the effect of distinct HF acid etching regimens on the biaxial flexural strength of a low-fusing nanofluorapatite glass-ceramic, (2) to study the ability of an UR to restore the initial (i.e., before etching) mechanical

properties, and (3) to evaluate the effect of HF acid etching on the ceramic surface morphology before and after UR treatment by scanning electron microscopy (SEM).

HYPOTHESES

The null hypotheses of this study were: (1) HF acid etching time would not decrease the biaxial flexural strength of the glass-based veneering ceramic tested, (2) the biaxial flexural strength of etched glass-based veneering ceramic would not be restored by UR treatment, and (3) the ceramic surface morphology would not be impaired by UR treatment.

REVIEW OF LITERATURE

DENTAL CERAMICS – A BRIEF OVERVIEW

Dental ceramics consist of both a glassy phase and a crystalline phase, and are generally categorized either by composition or fabrication technique (TABLE I). They can also be classified depending on their clinical applications into core or substructure and esthetic or veneering ceramics. Polycrystalline, crystalline and low-glass content ceramics with fillers are grouped into the core ceramics category. While glass-based and low filler(s) content ceramics are gathered as esthetic or veneering ceramics.^{1, 21, 22}

Core ceramics

The development of so-called core ceramics was achieved by increasing the volume percentage of the crystalline phase along with decreasing the glassy phase or even by excluding it.^{21, 22} The increased amount of crystalline phase is responsible for the mechanical properties improvement. Alumina- and zirconia-based ceramics are reinforced ceramics and have been used as core materials for crowns, FDPs, abutment as well as framework for dental implant-supported restorations due to high mechanical properties.²¹⁻²³ Among them, zirconia or zirconium dioxide ceramic is the most recent development for restorative dentistry. Indeed, the most common and often used zirconia is the 3-mol% yttria-containing tetragonal zirconia polycrystalline (3Y-TZP). Mechanical properties of zirconia are higher than all other dental ceramics, with flexural strength range from 900 - 1200 MPa, compressive strength ~ 2000 MPa and fracture toughness of

6-10 MPa. $m^{1/2}$.²⁴ Unfortunately, these are usually associated with high opacity and limitations regarding internal characterization or customized shading.

Veneering Ceramics

Veneering ceramics or esthetic ceramics consist of glass-based ceramics with or without fillers. This category is usually utilized for PLV, inlays, onlays, crowns and anterior FDPs, and it cannot be used for posterior long span restorations because of their generally low strength.

Glass-based Ceramics

Glass-based ceramics contain mainly silica dioxide also surrounded with various amounts of aluminum oxide. This group is recognized as feldspathic porcelain or aluminosilicate glasses.²¹ Regarding the mechanical properties of these materials, the flexural strength (three-point bending test) of two feldspathic veneering ceramics, i.e., Vitadur-Alpha and Vita VM7 (Vita-Zahnfabrik, Bad Säckingen, Germany) were investigated and reported at 57.8 ± 12.7 and 63.5 ± 9.9 MPa, respectively.^{25,26} On the other hand, the flexural strength of Vitabloc Mark II (Vita-Zahnfabrik), a feldspathic machinable block was found to be considerably greater ~ 154 MPa, most probably due to the ceramic chemical composition and processing technique.¹ It is well-known that feldspathic ceramics have low strength, and so these materials are usually being used in the fabrication of PLV, inlays, onlays and as veneering material over metal substructures or core ceramics.

Particle Filled Glass-based Ceramics

Several filler particles have been added to glass-based ceramics in order to increase the mechanical properties and the optical effects such as opalescence, translucence and color. The primary fillers used today are leucite, lithium disilicate or fluorapatite. The strength of ceramics materials have shown a significant increase after appropriate filler addition and uniform dispersion throughout the glass as per the dispersion strengthening mechanism.²¹

Leucite-containing Ceramics

Leucite-containing ceramics can be fabricated by adding higher amounts of potassium oxide to the aluminosilicate glassy phase. Leucite has a very high thermal expansion coefficient, CTE ($\sim 20 \times 10^{-6}/^{\circ}\text{C}$) compared to feldspathic ceramics ($\sim 8 \times 10^{-6}/^{\circ}\text{C}$). Thermally metal-compatible ceramics can be processed by adding leucite particles about 17 to 25% of the glass content (CTE for dental alloys $\sim 12-14 \times 10^{-6}/^{\circ}\text{C}$). Leucite is also used for dispersion strengthening by enhancing 40 to 55 % of leucite to glass phase.²¹ The most widely used commercially available dental ceramic in this group is IPS Empress (Ivoclar-Vivadent), but there are several other ceramics in this group such as Optimal Pressable Ceramic (OPC, Pentron, Wallingford, CT) and Empress Esthetic (Ivoclar-Vivadent).^{21, 23} According to the literature, the flexural strength of these materials range from 134-160 MPa.^{1, 27}

Lithium Disilicate Ceramics

Lithium disilicate glass-based ceramics have been introduced in the dental market aiming to achieve a high level of strength but still maintain the good esthetics and biocompatibility, two great advantages of glass-based ceramics. Lithium disilicate ceramics are fabricated by including lithium oxide into the aluminosilicate glassy phase. These materials were launched under the name IPS Empress 2 (Ivoclar-Vivadent) and the most recent brands are IPS e.max Press and IPS e.max CAD (Ivoclar-Vivadent). The IPS Empress 2 system has demonstrated higher flexural strength when compared to its predecessor (IPS Empress) Indeed, Albakry et al.²⁸ reported the biaxial flexural strength of IPS Empress 2 (Ivoclar-Vivadent) at 407 ± 45 MPa, whereas the leucite-containing ceramic (IPS Empress, Ivoclar-Vivadent) presented a considerably lower strength (175 ± 32 MPa). Correspondingly, Zogheib et al.²⁹ reported a similar biaxial flexural strength of 417 ± 55 MPa for IPS e.max CAD (Ivoclar-Vivadent). Based on that, the relatively good mechanical properties of lithium disilicate ceramic has supported its use for inlays, onlays, PLV, anterior and posterior crowns, 3-unit anterior and premolar FDPs and implant restorations.³⁰

Fluorapatite Ceramics

Concurrently, IPS e.max system has been developed (Ivoclar-Vivadent, Schaan, Liechtenstein) and used as a veneering material based on a low-fusing nanofluorapatite-based glass-ceramics (IPS e.max Ceram or IPS e. max ZirPress, Ivoclar-Vivadent) over lithium disilicate and zirconia frameworks in the fabrication of all-ceramic restorations.

According to the manufacturer, fluorapatite crystals ($\text{Ca}_5(\text{PO}_4)\text{F}$) of approximately 300 nm in length and about 100 nm in diameter govern the esthetic characteristics of this ceramic such as opalescence and translucence. Overall, fluorapatite glass-based ceramics can be either used to characterize and veneer IPS e. max restorations or can be used as PLV. There are two fabrication methods for fluorapatite glass based ceramics. IPS e.max ZirPress is heat pressed ceramic while IPS e.max Ceram is fabricated by the powder and liquid system. The manufacturer claims that the heat-pressed fluorapatite glass-based ceramic can generate restoration of even thickness, improve the homogeneous of the restoration in term of porosity, which in turn could also enhance the bond durability between ceramic restorations and teeth.³¹⁻³³ Guess et al.¹ reported the flexural strength of IPS e.max ZirPress at 110 MPa and 90 ± 10 MPa for IPS e.max Ceram according to the ISO 6872. Junpoom et al.³³ reported the mean flexural strength of IPS e.max Ceram at 78.6 ± 11.97 MPa by using three point bending test. In the same year, Choi et al.³⁴ utilized the piston-on-three-ball test on IPS e.max ZirPress and reported similar flexural strength values (89.6 ± 16.2 MPa).

EFFECT OF SURFACE CONDITIONING ON GLASS-BASED CERAMIC MICROSTRUCTURE

Bottino et al.⁸ reported qualitatively the changes in terms of ceramic surface topography after different surface conditioning methods such as HF acid etching and alumina air-abrasion. SEM images revealed that the ceramic surfaces of a high alumina ceramic (In-Ceram Alumina, Vita-Zahnfabrik) and a glass-based ceramic (Vitadur Alpha, Vita-Zahnfabrik) following air-abrasion with aluminum oxide presented sharp edges and

fragments of abrasive agent after air-abrasion. Ayad et al.¹¹ compared the effect of HF acid etching, orthophosphoric acid etching and aluminum oxide air-abrasion on the surface roughness and bond strength of a leucite-containing ceramic (IPS Empress, Ivoclar-Vivadent). Etching with HF acid generated irregularities and porosities that produced the highest bond strength, while the airborne particle abrasion with alumina did not create a retentive ceramic profile, although it was substantially rougher. Similarly, Torres et al.³⁵ stated the highest micro-shear bond strength of a lithium disilicate ceramic (IPS Empress 2, Ivoclar-Vivadent) was obtained when HF acid treatment was done followed by airborne particle abrasion treatment. The SEM micrographs revealed that the HF acid etching affected the surface of IPS Empress 2 (Ivoclar-Vivadent) by generating elongated crystals with shallow irregularities. In the same line of reasoning, a recent study by Naves et al.⁹ evaluated the effect of different HF acid etching times on the surface morphology and bond strength of a leucite-containing ceramic (Empress Esthetic, Ivoclar-Vivadent) with or without unfilled resin application after silane treatment. The results showed that the resin bond strength to ceramic decreased with increased HF etching times. More importantly, the ceramic specimens treated with silane and unfilled resin provided higher bond strength than specimens treated with silane alone.

Undoubtedly, one of the major factors that influence the success of dental restorations is related to its mechanical properties. Although various studies have reported on the improvement of the bond strength between resin-based cements and HF-etched glass ceramics, few studies have reported on the potential deleterious effect of the glassy-phase removal on the ceramic mechanical properties (e.g., flexural strength).

Therefore, a summary of the recent findings in the field are reviewed below in order to provide context for the present work.

HF ACID ETCHING ON GLASS-BASED CERAMIC MECHANICAL PROPERTIES

Yen et al.⁴ investigated the influence of HF acid etching on the flexural strength (three-point bending flexural test) of a feldspathic (Mirage, Myron International, Kansas City, KS) and a castable (Dicor, Dentsply, York, PA) glass-ceramics. The ceramics were allocated into five groups (n=10) according to the etching regimes, as follows: non-etched, 30 s, 60 s, 2.5 min and 5 min. It was found that the alteration of porcelain surfaces by HF acid etching at different etching regimens did not negatively impact the strength of either the ceramics tested. The mean flexural strength of the feldspathic ceramic ranged from 50.65 MPa to 56.29 MPa, while the castable glass-ceramic revealed a considerably higher strength ranging from 81.01 MPa to 86.76 MPa. Similarly, Thompson et al.³⁶ evaluated the flexural strength of a castable glass-ceramic (Dicor, Dentsply) after surface conditioning with 10% ammonium bifluoride (NH_4HF_2) for 1 min. Biaxial flexural test was performed on disc-shaped specimens (15 mm in diameter and 1.6 mm in thickness) using a piston-on-three-ball fixture. The authors reported that the use of NH_4HF_2 had no significant influence on the flexural strength between non-etched (80.9 ± 8.4 MPa) and etched specimens (84.2 ± 11.2 MPa).

On the other hand, Addison et al.⁷ evaluated the impact of various HF acid concentrations (5, 10 and 20%) and different etching times (45, 90 and 180 seconds) on the biaxial flexural strength of disc-shaped (15 mm \times 0.9 mm) feldspathic ceramic (Vitadur Alpha, Vita-Zahnfabrik) specimens on a ball-on-ring test set up. The mean

flexural strength of as-polished specimens and treated with 5, 10 and 20% HF acid were 94.4 ± 9.9 MPa, 83.4 ± 11.4 MPa, 84.9 ± 13.8 MPa, and 72.9 ± 11.2 MPa, respectively. While the mean flexural strength did not reveal the effect of the selected etching regimes; however, it changed the reliability of strength data. The authors suggested that both HF acid concentration and etching time have somewhat a weakening effect to the strength of the feldspathic ceramic.

Hooshmand et al.³ also noticed that HF acid etching significantly decreased the biaxial flexural strength of a leucite-containing (IPS Empress, Ivoclar-Vivadent) and a lithium disilicate ceramic (IPS Empress 2, Ivoclar-Vivadent). Disc-shaped specimens ($14 \text{ mm} \times 2 \text{ mm}$) were fabricated for each material. Then, half of the specimens in each group were etched with 9% HF acid for 2 minutes, while the remaining half served as control. The biaxial flexural strength was obtained after performing a piston-on-three-ball test. The results indicated HF acid reduced the strength for both ceramics as follows: IPS Empress (Ivoclar-Vivadent) (non-etched = 118.6 ± 25.5 MPa, etched = 102.9 ± 15.4 MPa) and IPS Empress2 (Ivoclar-Vivadent) (non-etched = 283 ± 48.5 MPa, etched = 250.6 ± 34.6 MPa). Furthermore, SEM micrographs revealed irregular pattern and extensive ceramic surface disruption from the invasive effect of HF acid.

In a recent study, Zogheib et al.²⁹ assessed the surface roughness and the flexural strength (three-point bending test) of a lithium disilicate glass-based ceramic (IPS e.max CAD, Ivoclar-Vivadent) after HF acid (4.9%) etching at four different etching regimens (20, 60, 90 and 180 seconds). All etching regimens created substantially rougher surfaces when compared to the non-etched group. The mean flexural strength values (MPa) of control group and 20, 60, 90 and 180 seconds etching time were: 417 ± 55 ; 367 ± 68 ; 363

± 84 ; 329 ± 70 ; and 314 ± 62 , respectively. The authors concluded that even though increasing the HF etching time increased the ceramic surface roughness it significantly decreased its flexural strength.

Similarly, one of the aims of this study was to investigate the effect of HF acid etching on the biaxial flexural strength of a glass-based ceramic (IPS e.max Zirpress, Ivoclar-Vivadent) after different etching regimens. Furthermore, the applicable HF acid etching time was determined over again even there is the guideline from manufacturer. However, some situations in clinical practice (e.g., saliva contamination) are difficult to follow the guideline and some studies^{6, 16, 37} showed the dissimilar etching regimens from the manufacturers. After this, the ability of UR to restore the biaxial flexural strength of IPS e.max ZirPress was investigated and SEM was used to evaluate the surface morphology of specimens before and after UR treatment.

MATERIALS AND METHODS

CERAMIC SPECIMENS PREPARATION

One hundred and forty four disk-shaped IPS e.max ZirPress ceramic specimens (15 ± 1 mm in diameter and 0.8 ± 0.1 mm in thickness) (FIGURE 1) were made from green casting wax (Corning's wax, Ronkonkoma, NY). The molds used to obtain the wax patterns were fabricated by adding the sprue wax to the wax patterns and then attached them to the sprue former (FIGURES 2-4). In order to measure the wax patterns dimensions, i.e., diameter and thickness, a digital caliper (Mitutoyo Digimatic Caliper, Mitutoyo Corp, Tokyo, Japan) was used. Investing was carried out using 200 g of IPS PressVEST Speed powder (Ivoclar-Vivadent) together with 32 mL of IPS PressVEST Speed liquid (Ivoclar-Vivadent) (FIGURE 5) and 22 mL of distilled water. Investment mixing was done under vacuum, for 2.5 minutes and then poured into the ring with slight vibration using a dental vibrator. After investment setting (~ 30 min), the silicone ring and sprue former were removed and the investment ring was transferred to the burn-out furnace at 850°C . After the burn-out process (~ 60 min), the investment ring was taken out from the furnace and the cold IPS e.max ZirPress ingot (FIGURE 6) and alumina plunger were inserted into the hot investment ring. The complete investment ring was transferred to the ceramic furnace Programat EP 5000 (Ivoclar-Vivadent) (FIGURE 7) and the e.max Zirpress program selected (TABLE II). After completion of the pressing stage, the investment ring was removed from the Programat 5000 and let it cool down to room temperature (FIGURE 8). Once cooled, the investment was divested from the

specimen with polishing glass beads: first at 4 bars (60 psi) and then at 2 bars (30 psi) of pressure. All the specimens were cleaned with Invex liquid (Ivoclar-Vivadent) and running water. The specimens were wet-ground with 400-grit and 600-grit silicon carbide paper to obtain standardized flat surfaces, cleaned in an ultrasonic bath with distilled water for 15 minutes and then air-dried (FIGURE 9).

ETCHING PERIODS AND SURFACE TREATMENT

The fabricated disk-shaped IPS e.max ZirPress ceramic specimens were distributed into 12 groups (n=12) according to the etching regime (TABLE III). A 5% hydrofluoric acid gel (IPS ceramic etching gel, Ivoclar-Vivadent) (FIGURE 10A) was used, since this is the concentration recommended by the manufacturer. Group 1 was left as-polished (control), Groups 2-5 were etched at 30, 60, 90 and 120 seconds, respectively. Meanwhile groups 7-11 were treated similarly to groups 1-5 in the same order but a silane agent followed by the application of an UR was performed. For the re-etched groups (groups 6 and 12); which were intended to simulate saliva contamination (IRB #0304-58) before cementation, the samples were immersed in saliva at 37°C for 1 minute, then the specimens were rinsed with distilled water and air-dried before the second etching procedure. After etching, all groups were rinsed with distilled water for 20 s and air-dried for 10 s. All of specimens were placed in isopropyl alcohol followed by sonication for 60 minutes in order to ensure the elimination of not only contaminants such as grease and oil from handling, surfactant from acid gels and saliva³⁸ but more importantly the formed salts over the ceramic microstructure that could impede proper resin infiltration. In groups 7-12, a silane coupling agent (Silane Monobond S, Ivoclar

Vivadent) (FIGURE 10B) was applied on the surfaces for 60 s, air-dried, and coated with a single layer of an UR (Heliobond, Ivoclar Vivadent) (FIGURE 10C). A single layer of the UR was validated by the following: firstly, one drop of the unfilled resin solution was placed into a mixing well. Secondly, a microbrush was dipped into the resin and then applied to the etched ceramic surface. Thirdly, polymerization through a Mylar strip was carried out for 10 seconds (FIGURE 11). Lastly, the individual thickness of the specimens from groups 7-12 was measured using a digital caliper (Mitutoyo Digimatic Caliper, Mitutoyo) after specimen preparation. The specimens of G1-G6 were etched on the same day as the biaxial flexural test performed, while ceramic surface of G7-12 specimens were conditioned 24 hours prior to the test and stored in a desiccator at 37°C with a relative humidity of 16% before testing.

SURFACE MICRO-MORPHOLOGY EVALUATION

One additional specimen per group was fabricated for SEM qualitative evaluation. The specimens were mounted on Al stubs, sputter-coated with Au-Pd alloy (FIGURE 12) and imaged at different magnifications using a JEOL SEM (JSM-6390, JEOL, Tokyo, Japan) (FIGURE 13) at an acceleration voltage of 3-5 kV. The working distance and spot size were set at 10 mm and 30, respectively.

BIAXIAL FLEXURAL STRENGTH TEST

IPS e.max ZirPress (Ivoclar-Vivadent) biaxial flexural strength of the different groups tested (G1-G12) were determined by using a piston-on-three-ball technique as per ISO 6872. Briefly, after centering the disk-shaped IPS e.max ZirPress specimens on the

top of three steel spheres (i.e., 3.2 mm in diameter, 120° apart forming a circle of 10 mm diameter) (FIGURES 14 and 15) , a 50 kgf load at a rate of 1 mm min⁻¹ was applied perpendicular to the center of the specimens by the circular cylinder steel with a 1.58 mm diameter flat-end tip using a universal testing machine until fracture (MTS Sintech ReNew 1123, Eden Prairie, MN) (FIGURES 16-19).²⁶ Biaxial flexural strength was calculated based on the recorded load at fracture using the standard equation, as shown below:

$$S = -0.2387P(X - Y)/d^2,$$

where: S is the maximum tensile stress (in MPa) and the biaxial flexural strength at fracture, P is the load at fracture (in N), and d is the specimen thickness at fracture origin (in mm).

$$X = (1+\nu) \ln (B/C)^2 + [(1 -\nu)/2] (B/C)^2,$$

$$Y = (1+\nu) [1 + \ln (A/C)^2] + (1 -\nu) (A/C)^2$$

where: ν is the Poisson's ratio, A is the support ball radius (mm), B is the radius of the tip of the piston (mm), and C is the specimen radius (mm). A 0.25 Poisson's ratio was used since it is considered the standard recommendation.^{26, 39-42}

WEIBULL STATISTICS

The Weibull analysis was performed on the ascending order ranking of the biaxial flexural strength data. The Weibull distribution followed the equation:

$$Pf = 1 - \exp \left[- \left(\frac{\delta}{\delta_{n0}} \right)^m \right]$$

Where Pf is the probability of failure, δ is the strength at a given Pf , δn_0 is the characteristic strength, and m is known as Weibull modulus. Pf was calculated from the following formula:

$$Pf = \frac{RANK}{(N+1)}$$

Where $RANK$ is the rank order of flexural strength and N is the total number of specimens. The Weibull distribution can be simplified as follows:

$$\ln \ln \left[\frac{1}{(1-Pf)} \right] = m \ln \delta - m \ln \delta n_0 \quad ^{39-41, 43}$$

STATISTICAL METHODS

Summary statistics (mean, standard deviation, standard error, range) were calculated for ceramic flexural strength data for each of the twelve groups. Statistical analysis using two-way ANOVA and Sidak multiple comparisons procedure were used to evaluate the effects of etching time and treatment with UR on the flexural strength data. In addition, the Weibull characteristic strength and modulus parameters were estimated using survival analysis. The significance level was set at 5%.

Based on previous studies³⁻⁷, the within-group standard deviation was expected to be 35 MPa for flexural strength. With a sample size of 12 specimens per group, the study would have 80% power to detect differences of 60 MPa for flexural strength, assuming two-sided tests conducted at an overall 5% significance level.

RESULTS

MICRO-MORPHOLOGICAL EVALUATION

SEM micrographs, at different magnifications, of the non-etched (G1) and etched ceramic surfaces (G2-G6) are presented in figures 20-31. Overall, the IPS e. max ZirPress ceramic surface became more porous, at various degrees in all etched groups.

Representative SEM micrographs of the as-polished group (G1) showed the presence of surface flaws (i.e., pores) (FIGURES 20 and 21). After HF etching for 30 s and 60 s (G2 and G3) smoother surfaces were observed when compared to G1 at low magnification ($\times 500$ and $\times 1500$). However, at higher magnification ($\times 3500$) both G2 and G3 revealed the presence of nano- and microporosities and fissures more than G1 even though these seemed to be shallower than G1 (FIGURES 22-25). A more irregular surface pattern (i.e., mixing of porosities, fissures and smooth areas) was seen in the 90 s HF etched group (G4) (FIGURE 26). Representative SEM micrograph at higher magnification clearly shows the dissolution of the glassy phase with the formation of precipitation salts and accentuated etching of the ceramic microstructure (FIGURE 27). For the 120 s and re-etched groups (G5 and G6) a similar pattern was observed when compared to G4, with the presence of pores of different sizes, precipitated salts, an evident etching of the substrate and numerous fissures extending throughout the ceramic microstructure. Furthermore, considerably larger etched areas (i.e., voids) can be seen at the re-etched ceramic group (G6) at higher magnification (FIGURES 28 - 31). Finally, the ultrasonic

cleaning method used was able to remove most of the salt remnants off the ceramic surface making the surface topography more evident (FIGURES 23 and 27).

Figures 32-37 show the SEM micrographs of the ceramic surfaces treated in the same fashion as G1-G6; but followed by silane and UR applications (G7-G12). Overall, representative SEM micrographs of UR treated surfaces revealed the penetration of the low viscosity resin into the porous surface, as can be demonstrated by the creation of a smooth, glass-like surface; except the areas presenting ceramic defects due to processing and areas of inadequate resin application (FIGURES 32, 33 and 35-37). An interesting surface pattern was observed for the ceramic etched with HF for 60 s (G9). The crystal fillers are higher than glassy phase areas that already got dissolved by HF acid treatment. Even though, the silane and UR penetrated into glassy phase of ceramic and also covered the crystal fillers, the different level between crystal fillers and glassy phase still can be seen.

BIAXIAL FLEXURAL STRENGTH

Means, respective standard deviations (\pm SD), standard errors (\pm SE) and ranges for biaxial flexural strength are presented in table IV and figure 38. For non-resin surface treated groups (G1 – G6), G4 had the highest mean flexural strength at 106.8 ± 21.7 MPa, whereas G6 presented the lowest mean flexural strength at 94.1 ± 11.9 MPa. Among the resin-treated groups (G7 – G12), G10 showed the highest mean flexural strength of 120.6 ± 16.8 MPa, while the lowest mean flexural strength of 101.5 ± 11.8 MPa was related to G7. Moreover, all of the resin-treated groups (G7 – G12) revealed superior mean flexural strength than non-resin treated groups at the same etching time (G1 – G6).

The two-way ANOVA followed by a pair-wise test using the Sidak multiple comparisons procedure for the experimental groups revealed that the etching time/surface treatment interaction was not significant ($p=0.40$). However, a significant effect of etching time ($p=0.0290$) on biaxial flexural strength was observed. Indeed, HF etching for 90 s (G4, 106.8 ± 21.7 MPa) led to a significantly ($p=0.0392$) higher mean flexural strength than control group (G1, 98.4 ± 14.9 MPa). Correspondingly, the 90 s of HF etching followed by unfilled resin treatment (G10) revealed a considerably higher mean flexural strength (120.6 ± 16.8 MPa) than the as-polished followed by resin treatment (G7) at 101.5 ± 11.8 MPa ($p=0.0392$). Furthermore, biaxial flexural strength was significantly higher for unfilled resin-treated surfaces (G7 – G12) than for untreated surfaces (G1 – G6) ($p<0.0001$).

WEIBULL STATISTICS

The Weibull distribution survival analysis was used to compare the differences in biaxial flexural strength between the tested groups. The Weibull distribution survival analysis used the stress required for failure instead of the usual “time to event” seen in typical survival analyses. The Weibull statistical parameters; Weibull characteristic strength (δn_0) and Weibull modulus (m) are also presented in Table V. For G1 – G6, G4 showed the highest Weibull characteristic strength at 115.6 MPa. On the contrary, the lowest Weibull characteristic strength of 99.3 MPa was seen in G6. In G7 – G12, the highest Weibull characteristic strength was presented in G10 at 128.1 MPa. By contrast, G7 had the lowest Weibull characteristic strength of 106.7 MPa. In addition, G7 – G12 showed higher Weibull characteristic strength than G1 – G6 for the same etching time.

Weibull moduli in this study range from 5.7 (G4) to 16.3 (G2). Figure 39 presents the survival curves fitted by the Weibull models; the y axis shows survival probability of failure from 1 to 0, where 1 means no failures and 0 is equal total failure of all the samples. The x axis represents biaxial flexural strength in MPa.

TABLES AND FIGURES

TABLE I

Dental ceramics classification

Composition	Fabrication Technique	Trade Name
Glass-based ceramic		
- Aluminosilicate glasses	Powder and liquid	Vita VM7, Vitadur Alpha, Noritake, Ceramco
Particle filled glass-based ceramic		
- Leucite	Powder and liquid	Vita VM9, 13,17, IPS Empress
	Heat pressed	Vita PM9, IPS Inline POM, OPC,
- Lithium disilicate	CAD/CAM	Empress Esthetic
	Heat pressed	ProCAD
		IPS e.max Press, IPS Empress2
	CAD/CAM	IPS e.max CAD
- Fluorapatite	Powder and liquid	IPS e.max Ceram
	Heat pressed	IPS e.max ZirPress
Crystalline-based ceramic with glass filler		
- Alumina	Slip casting, milled	In-Ceram
- Alumina/Zirconia	Slip casting, milled	In-Ceram zirconia
- Alumina/Magnesia	Slip casting, milled	In-Ceram Spinell
Polycrystalline ceramic		
- Alumina	Sintered	Procera
- Zirconia	CAD/CAM	IPS e.max ZirCAD, Lava, Cercon

TABLE II

Firing cycle of IPS e.max ZirPress according to manufacturer's recommendation

Material	Heat up temp (°C)	Start temp (°C)	Heat rate (°C/min)	Vacuum hold time (min)	Pressing temp (°C)	Press time (min)
IPS e.max ZirPress	900	700	60	15	910	6

TABLE III

Description of experimental groups

Groups	Etching Regimen	Surface Treatment
1	0	-
2	30	-
3	60	-
4	90	-
5	120	-
6	60+60	-
7	0	Silane + unfilled resin
8	30	Silane + unfilled resin
9	60	Silane + unfilled resin
10	90	Silane + unfilled resin
11	120	Silane + unfilled resin
12	60+60	Silane + unfilled resin

TABLE IV

Means (MPa) \pm SD, \pm SE and range of biaxial flexural strength of experimental groups

Group (N=12)	Etching Time (s)	Surface Treatment	Mean (MPA)	SD	SE	Min	Max
1	0	None	98.4	14.9	4.3	77.8	121.3
2	30	None	98.4	8.0	2.3	79.2	109.3
3	60	None	103.6	12.0	3.5	75.9	120.4
4	90	None	106.8	21.7	6.3	73.3	148.6
5	120	None	103.4	17.9	5.2	73.7	129.1
6	60+60	None	94.1	11.9	3.4	75.7	112.7
7	0	Resin	101.5	11.8	3.4	82.9	126.9
8	30	Resin	107.2	16.7	4.8	86.8	142.3
9	60	Resin	111.2	16.7	4.8	81.5	145.9
10	90	Resin	120.6	16.8	4.9	101.1	153.2
11	120	Resin	118.2	10.5	3.0	105.3	141.9
12	60+60	Resin	115.7	21.6	6.2	95.2	170.4

TABLE V

Flexural strength means (δ), and statistical parameters (δn_0 and m) obtained from the Weibull Distribution of the initial mechanical strength.

Group (N=12)	Etching Time (s)	Surface Treatment	Mean Flexural Strength (MPa)	Weibull Characteristic Strength (MPa)	Weibull Modulus
1	0	None	98.4	104.7	7.5
2	30	None	98.4	101.7	16.3
3	60	None	103.6	108.5	11.6
4	90	None	106.8	115.6	5.6
5	120	None	103.4	110.6	7.4
6	60 + 60	None	94.1	99.3	9.5
7	0	Resin	101.5	106.7	9.0
8	30	Resin	107.2	114.4	6.7
9	60	Resin	111.2	118.2	7.3
10	90	Resin	120.6	128.1	7.4
11	120	Resin	118.2	123.2	11.0
12	60 + 60	Resin	115.7	124.8	5.2

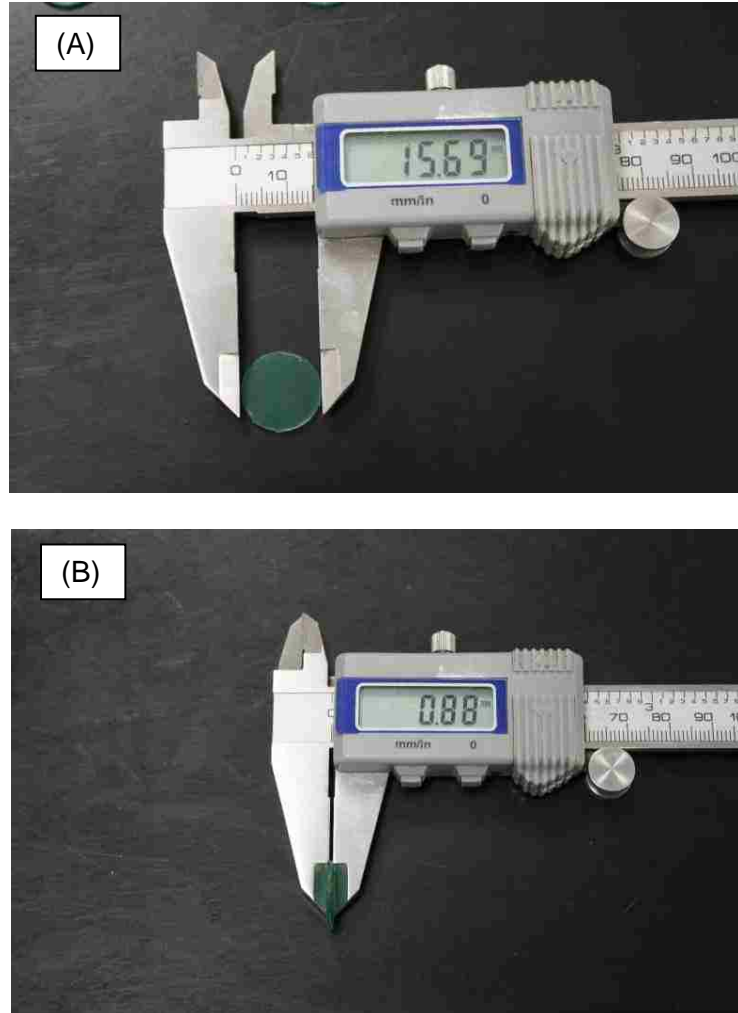


FIGURE 1. Demonstration of measurement of the wax pattern using a digital caliper

(A) Width in millimeters (mm), and (B) thickness.



FIGURE 2. Macro photograph of sprued wax patterns

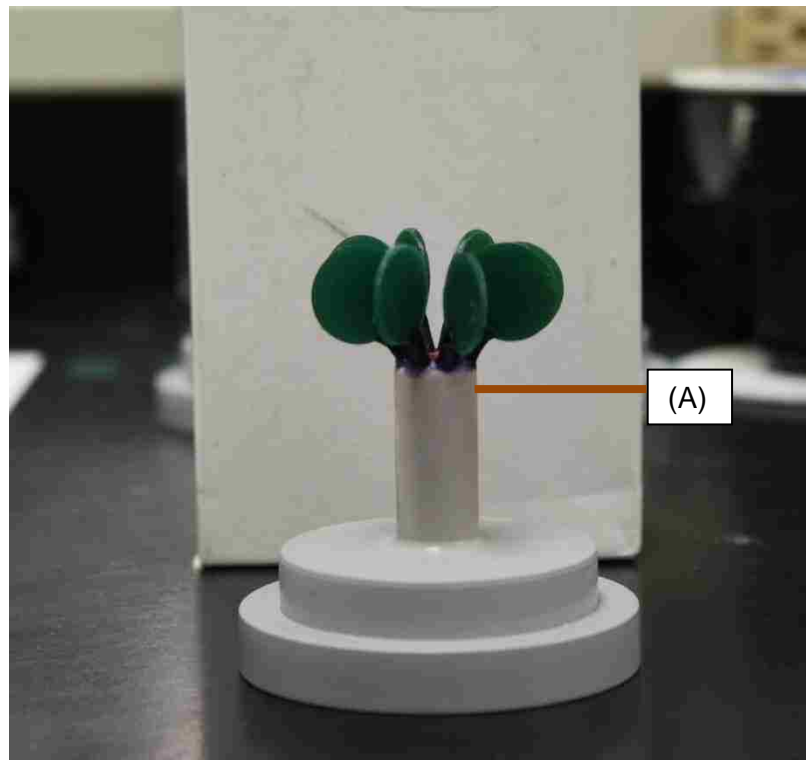


FIGURE 3. Illustration of wax patterns attached to the sprue former (A)

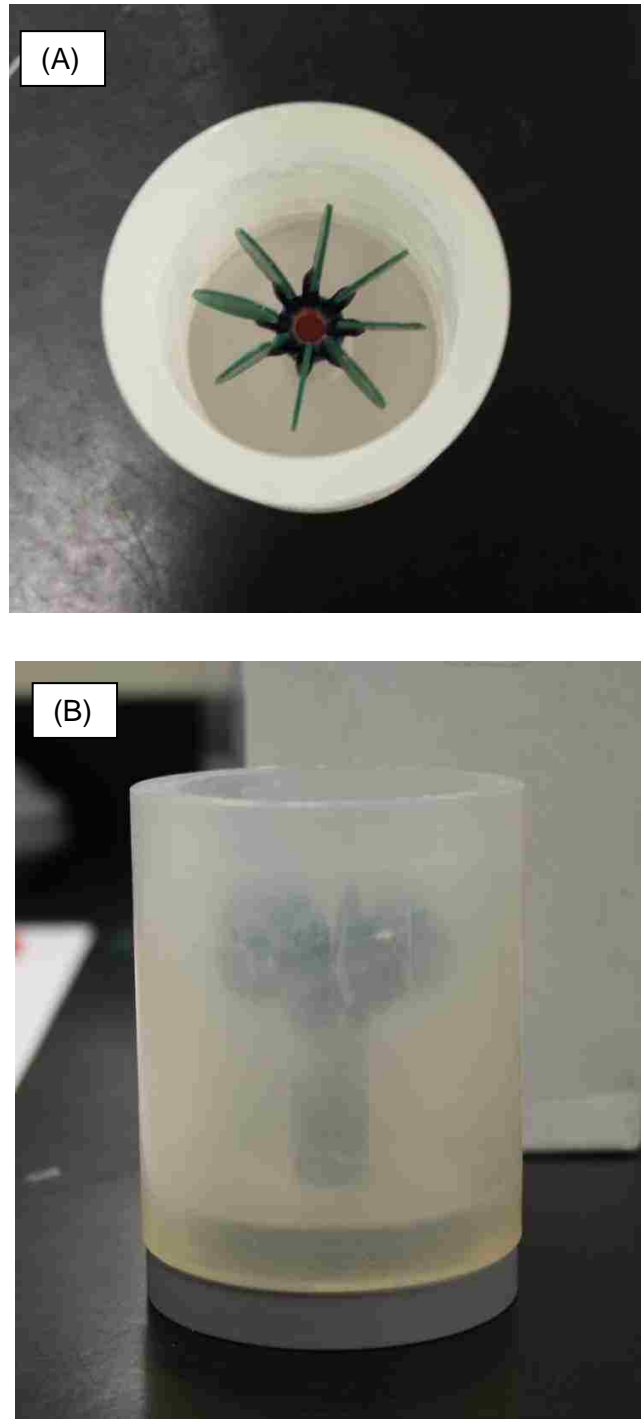


FIGURE 4. Macrophotographs of a wax pattern mold ready for investing;
(A) Top view, and (B) side view



FIGURE 5. IPS PressVest Speed powder and liquid (Ivoclar-Vivadent)



FIGURE 6. IPS e.max ZirPress ingots (Ivoclar-Vivadent)



FIGURE 7. Furnace Programat EP 5000 (Ivoclar-Vivadent) used for ceramic processing



FIGURE 8. Pressed investment rings



FIGURE 9. Representative of IPS e.max ZirPress (Ivoclar-Vivadent) polished ceramic specimens

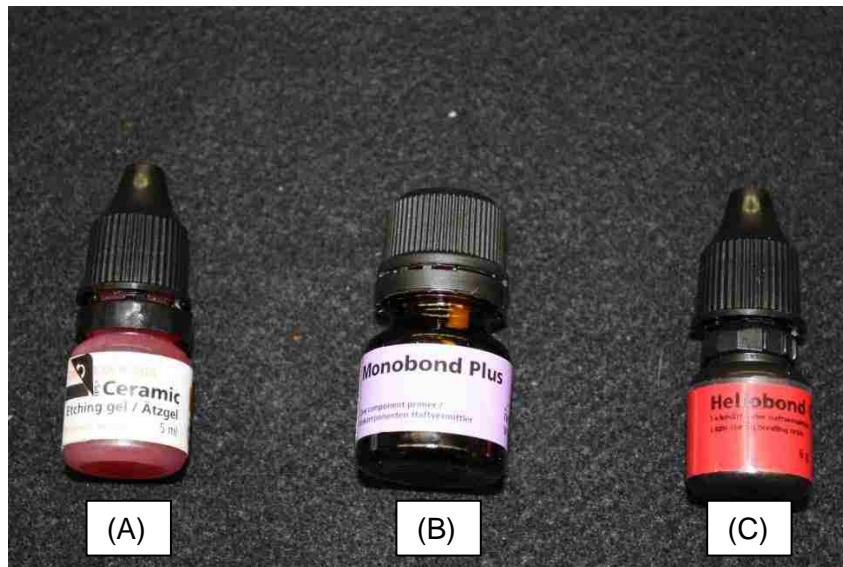


FIGURE 10. Macrophotographs of (A) IPS ceramic etching gel, (B) Monobond Plus, and (C) Heliobond (Ivoclar-Vivadent)

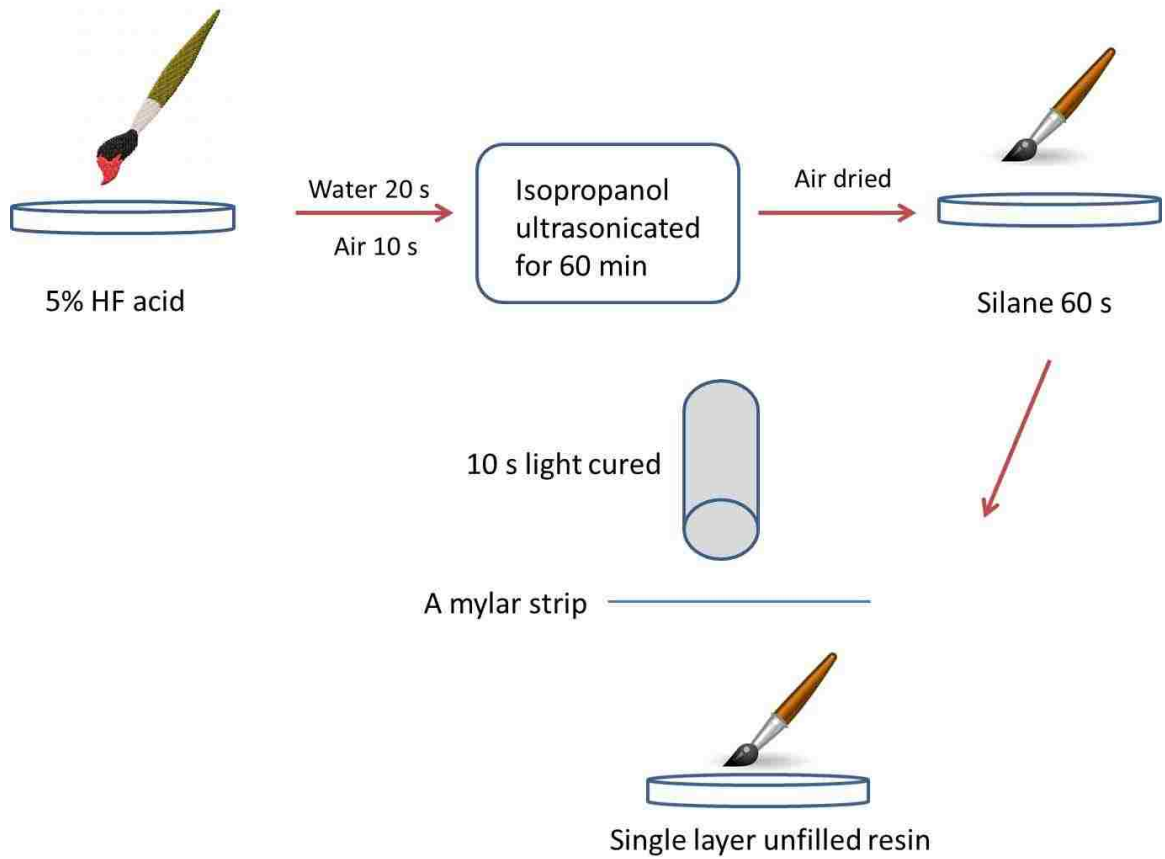


FIGURE 11. Schematic representation of the etching and surface treatment procedures



FIGURE 12. Illustration of specimens preparation for SEM



FIGURE 13. A JEOL SEM (JSM – 6390) used for surface micro-morphological evaluation

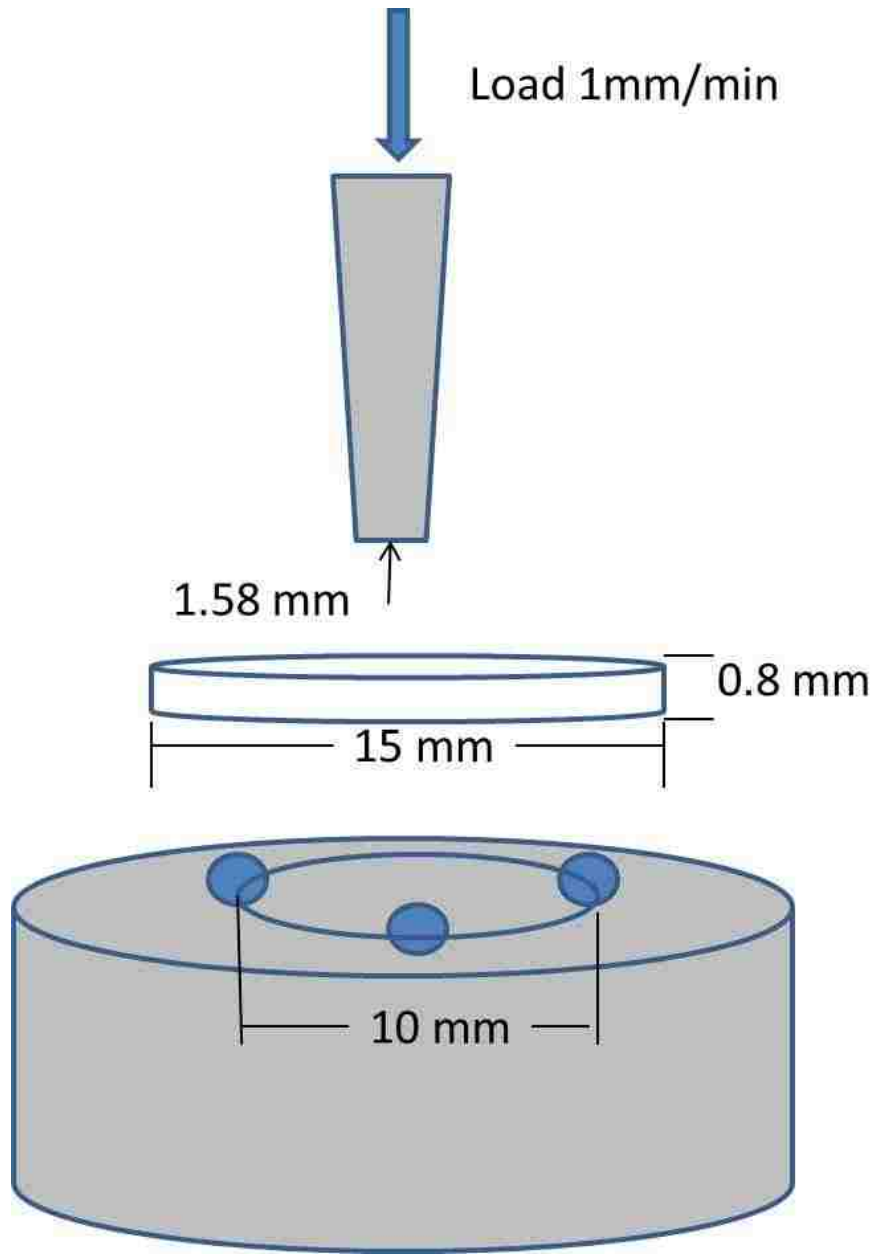


FIGURE 14. Schematic representation of a-piston-on-three-ball jig for biaxial flexural test



FIGURE 15. Illustration of a-three-ball-jig for biaxial flexural strength



FIGURE 16. A universal testing machine (MTS Sintech ReNew 1123) used for biaxial flexural test

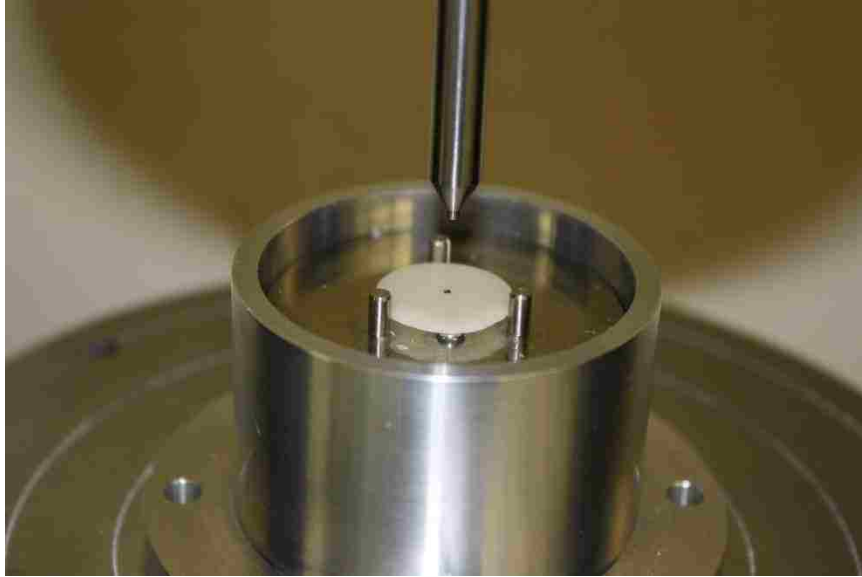


FIGURE 17. Illustration of ceramic specimen set up on a -three-ball jig



FIGURE 18. Illustration of ceramic specimen set up on a-three-ball jig and the position of a piston ready for loading



FIGURE 19. Illustration of ceramic specimen fracture after force loading

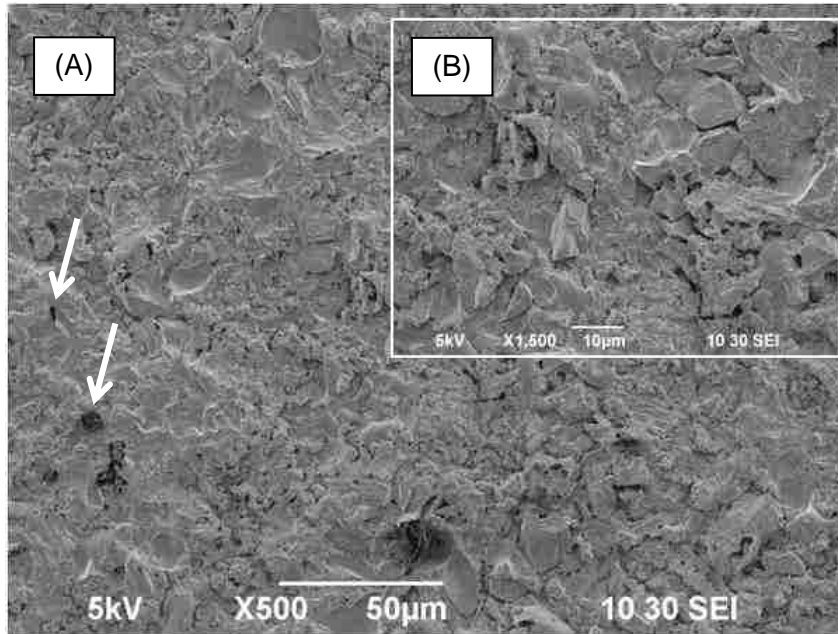


FIGURE 20. Representative SEM micrographs of the as-polished ceramic group (A) at $\times 500$ magnification, white arrows indicate pores and (B) at $\times 1500$ magnification.

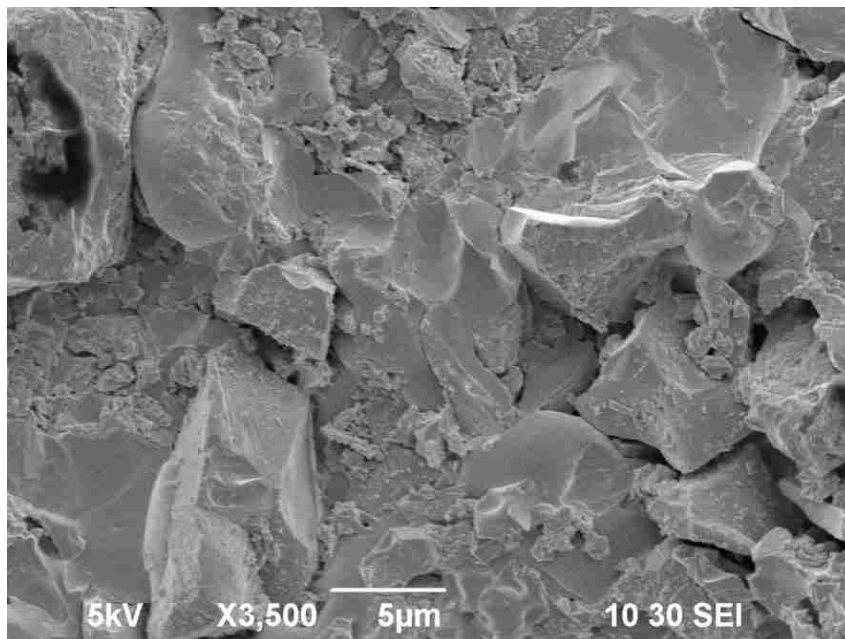


FIGURE 21. Representative SEM micrograph of the as-polished ceramic group at higher magnification ($\times 3500$).

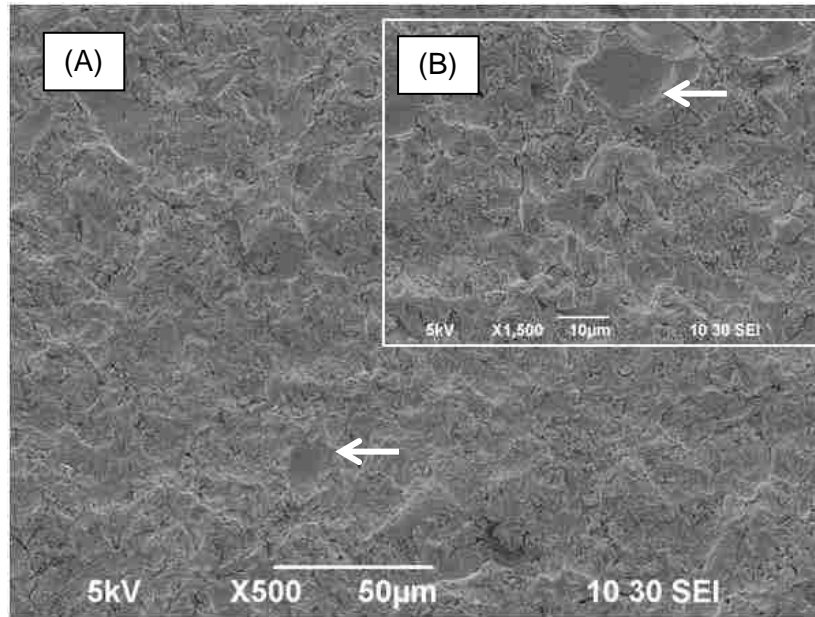


FIGURE 22. Representative SEM micrographs of the 30 s etched ceramic group (A) at $\times 500$ magnification and (B) at $\times 1500$ magnification. White arrows indicate smooth surface.

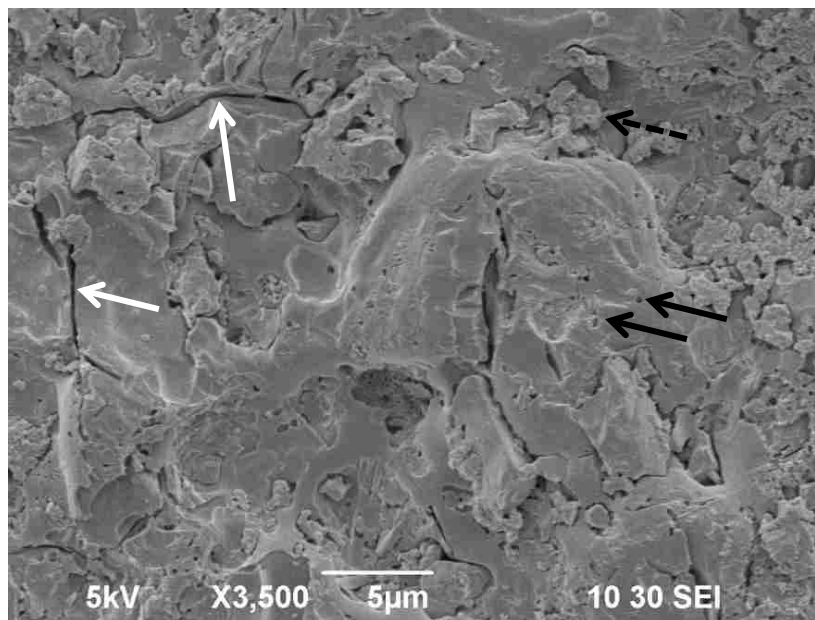


FIGURE 23. Representative SEM micrograph of the 30 s etched ceramic group at higher magnification ($\times 3500$) presents fissures (white arrows), microporosities (black arrows) and precipitated salts (dotted black arrow).

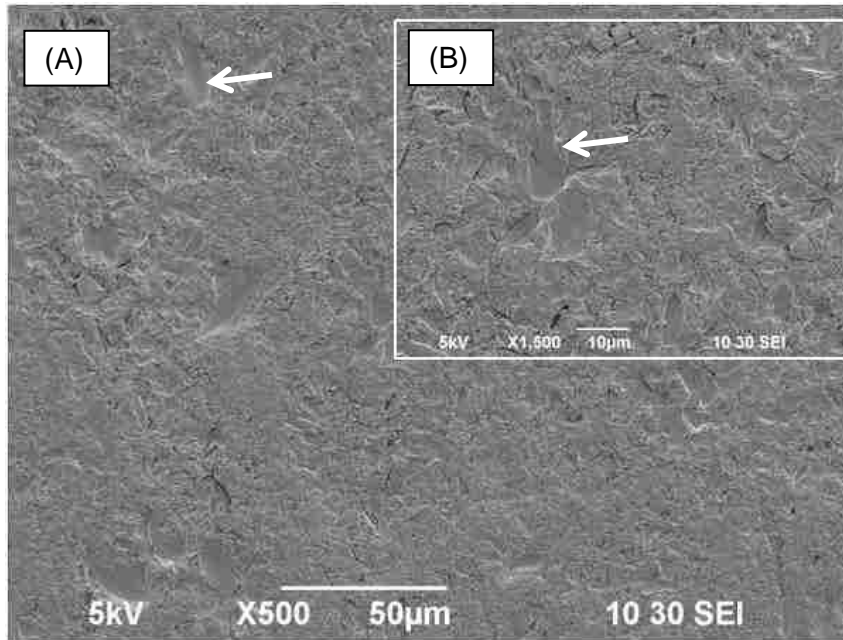


FIGURE 24. Representative SEM micrographs of the 60 s etched ceramic group (A) at $\times 500$ magnification and (B) at $\times 1500$ magnification. White arrows indicate smooth surface.

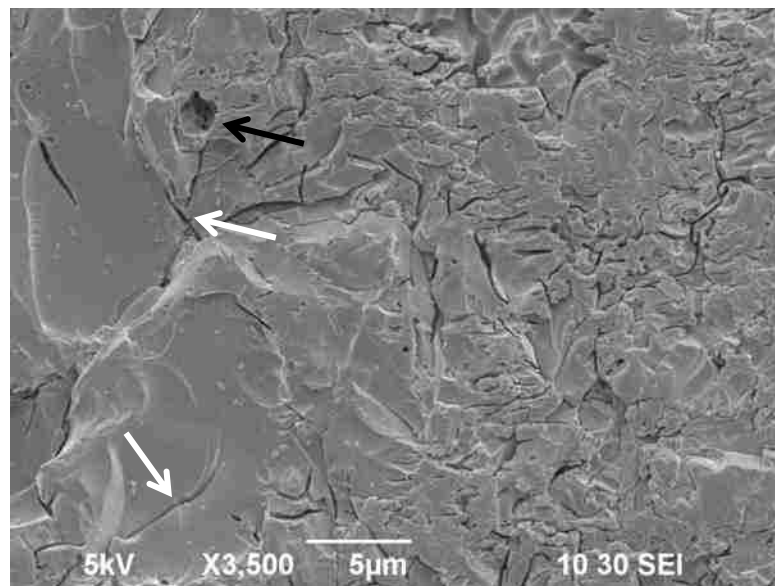


FIGURE 25. Representative SEM micrograph of the 60 s etched ceramic group at higher magnification ($\times 3500$) presents pores (black arrows) and fissures (white arrows).

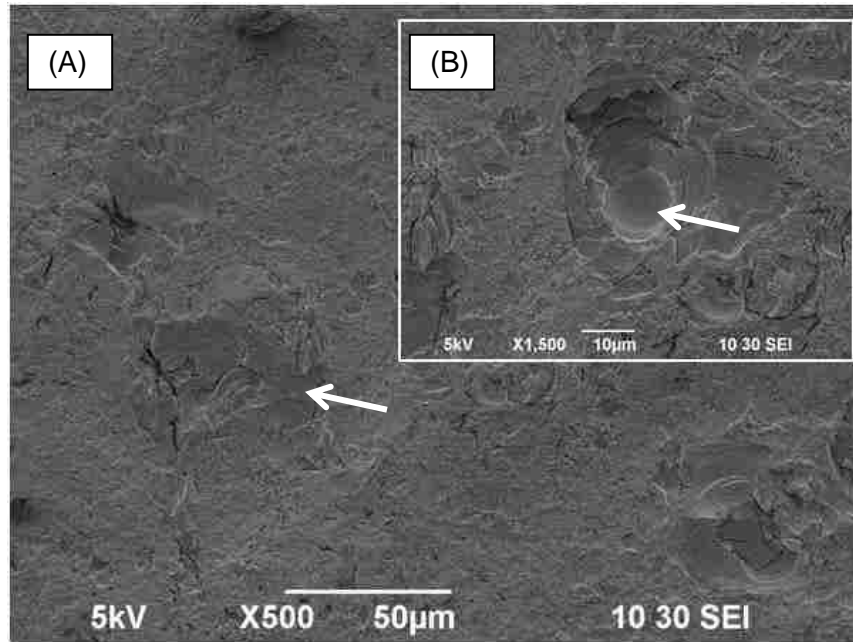


FIGURE 26. Representative SEM micrographs of the 90 s etched ceramic group (A) at $\times 500$ magnification and (B) at $\times 1500$ magnification. White arrows show smooth surfaces.

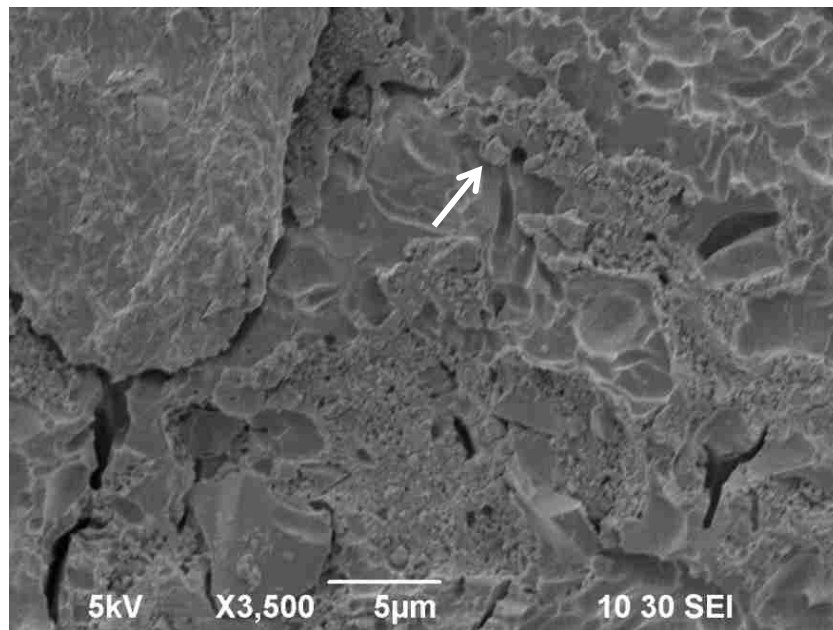


FIGURE 27. Representative SEM micrograph of the 90 s etched ceramic group at higher magnification ($\times 3500$) presents precipitated salts (white arrows).

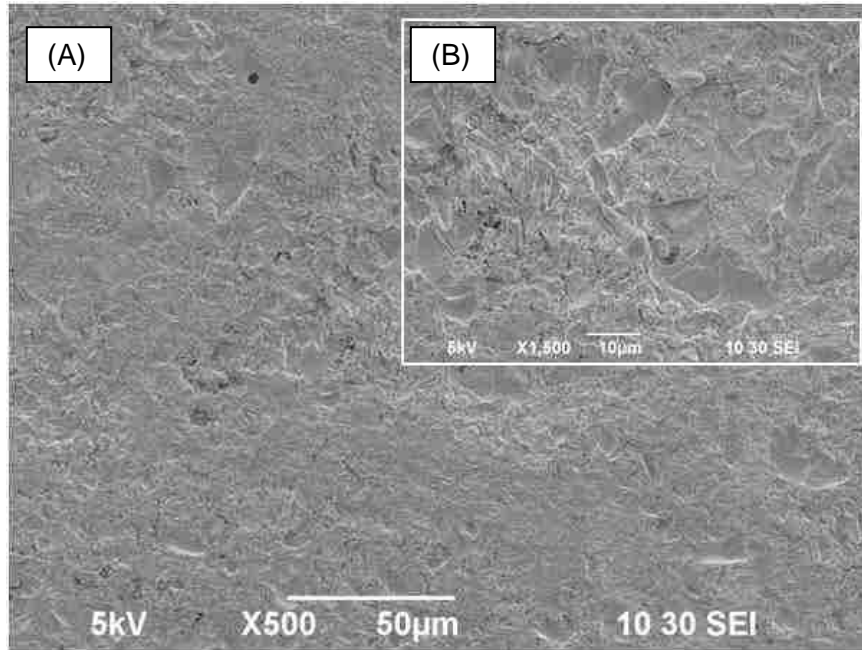


FIGURE 28. Representative SEM micrographs of 120 s etched ceramic group (A) at $\times 500$ magnification and (B) at $\times 1500$ magnification.

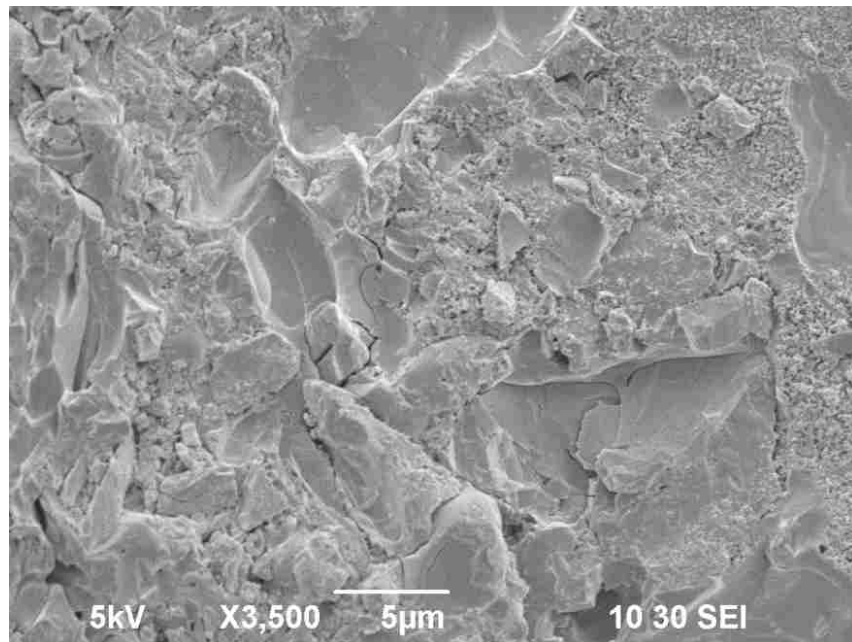


FIGURE 29. Representative SEM micrograph of 120 s etched ceramic group at higher magnification ($\times 3500$).

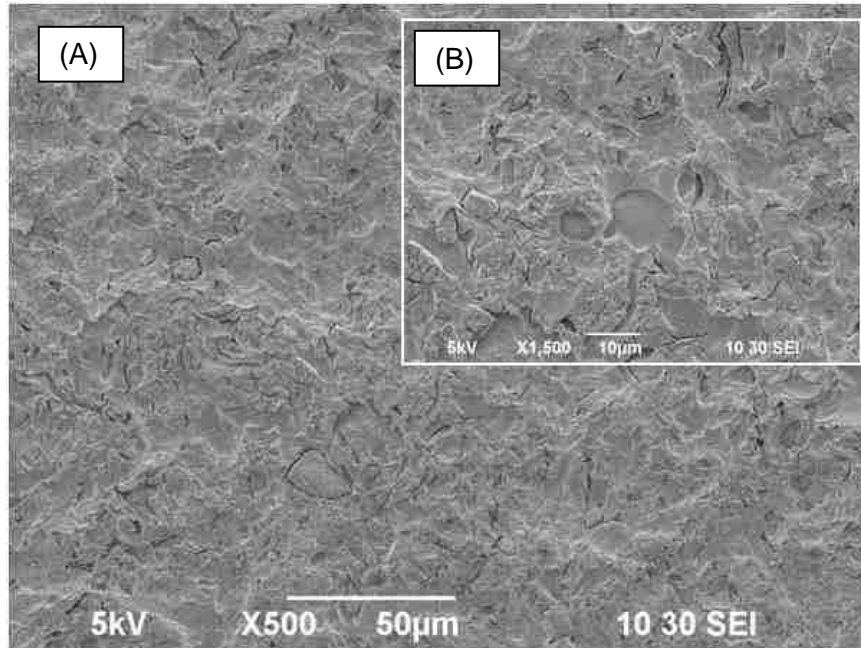


FIGURE 30. Representative SEM micrographs of re-etched ceramic group (A) at $\times 500$ magnification and (B) at $\times 1500$ magnification.

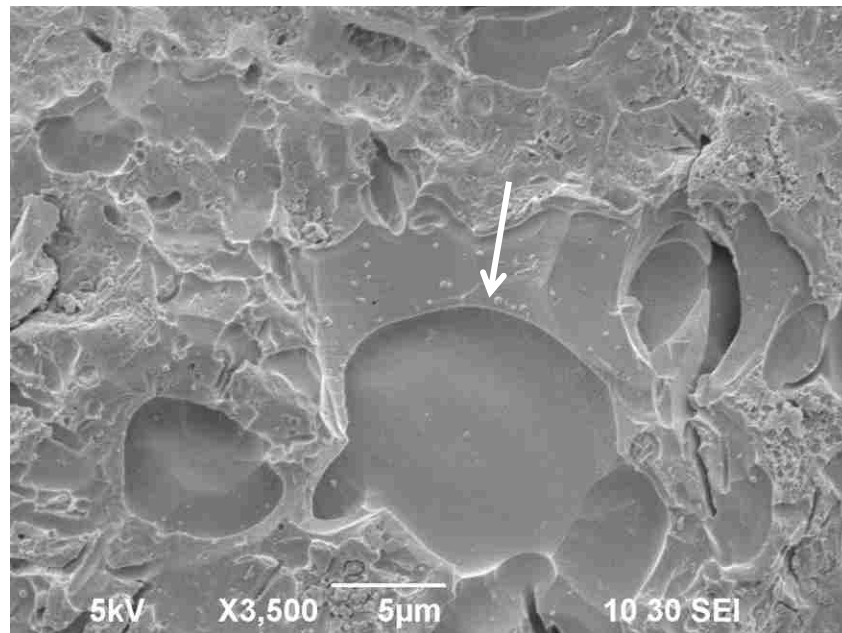


FIGURE 31. Representative SEM micrograph of re-etched ceramic group at higher magnification ($\times 3500$) shows voids (white arrow).

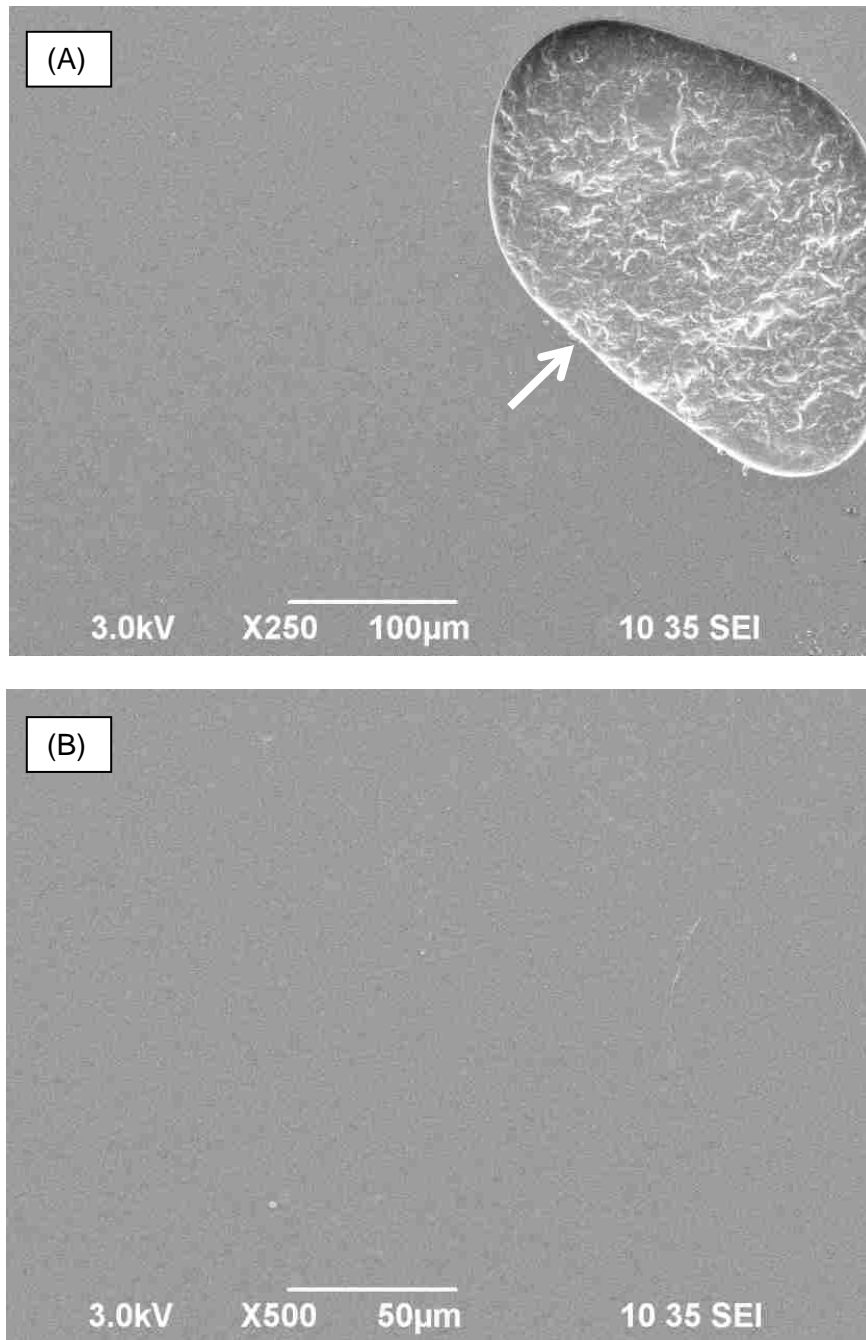


FIGURE 32. Representative SEM micrographs of as polished ceramic with UR application (A) at $\times 250$ magnification and (B) at $\times 500$ magnification.

The homogeneously smooth, glass-like surface, except for the presence of defects seen in white arrow.

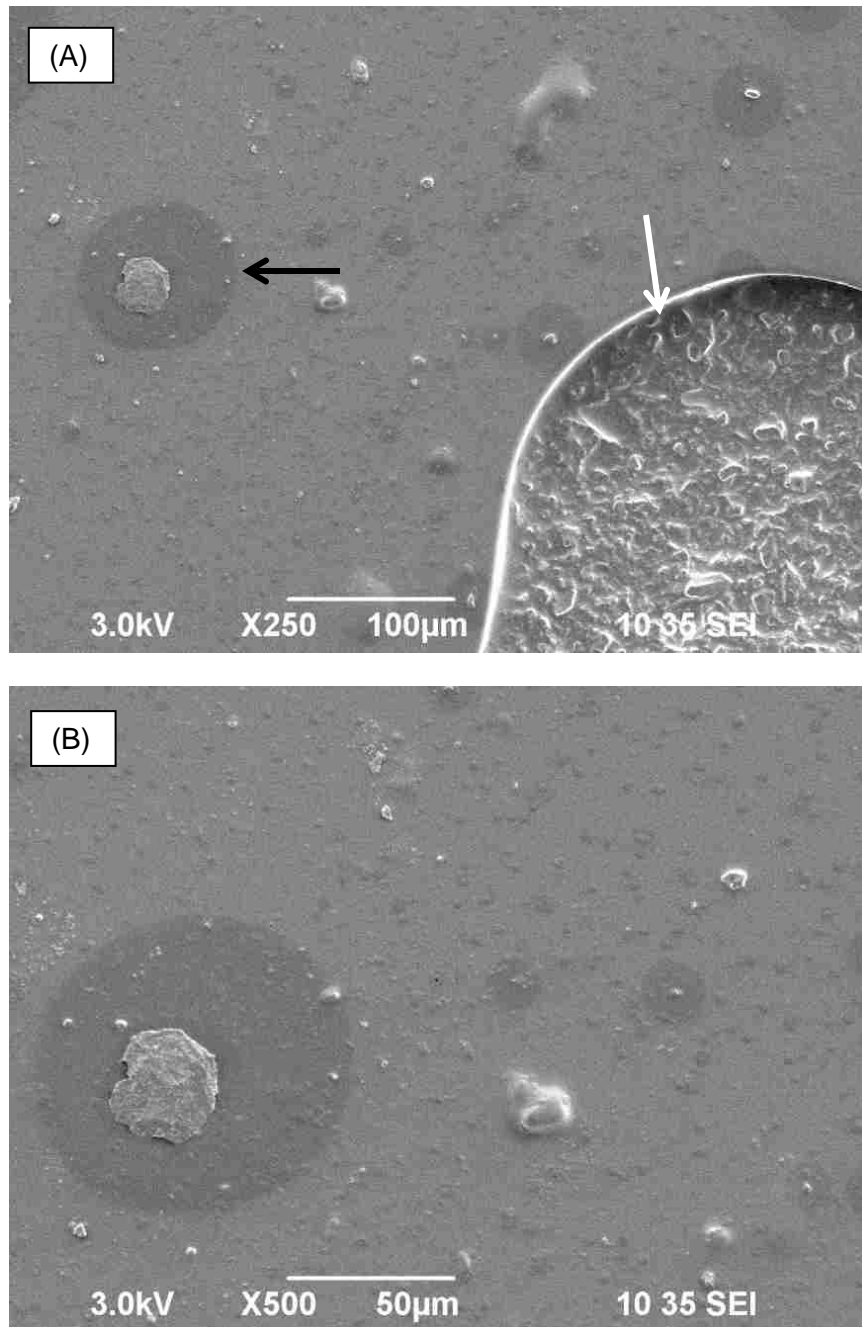


FIGURE 33. Representative SEM micrographs of 30 s etched ceramic with UR application (A) at $\times 250$ magnification and (B) at $\times 500$ magnification. White arrow indicates defect area and black arrow shows bubble.

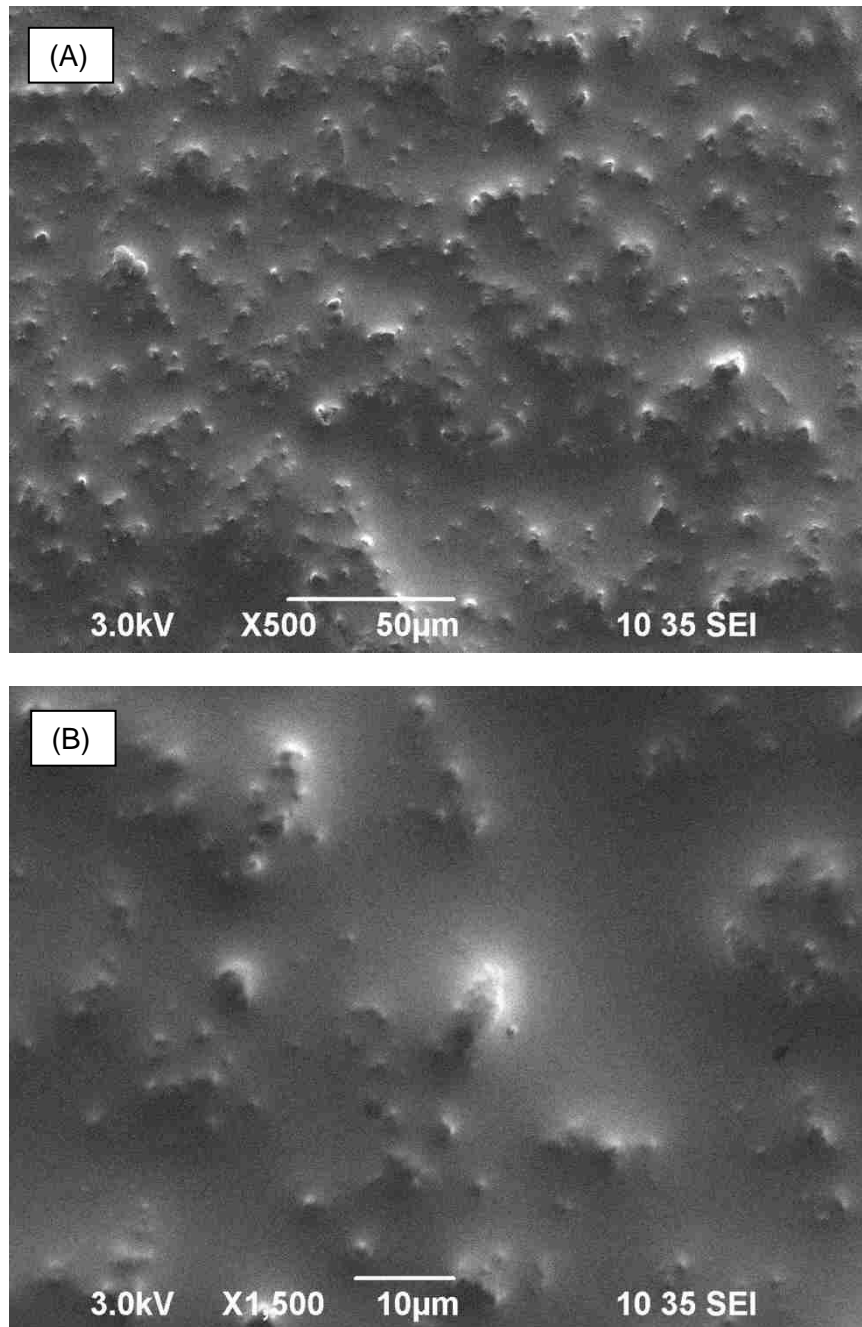


FIGURE 34. Representative SEM micrographs of 60 s etched ceramic with UR application (A) at $\times 500$ magnification and (B) at $\times 1500$ magnification. The different level of crystal fillers and glassy phase of ceramic is noticed.

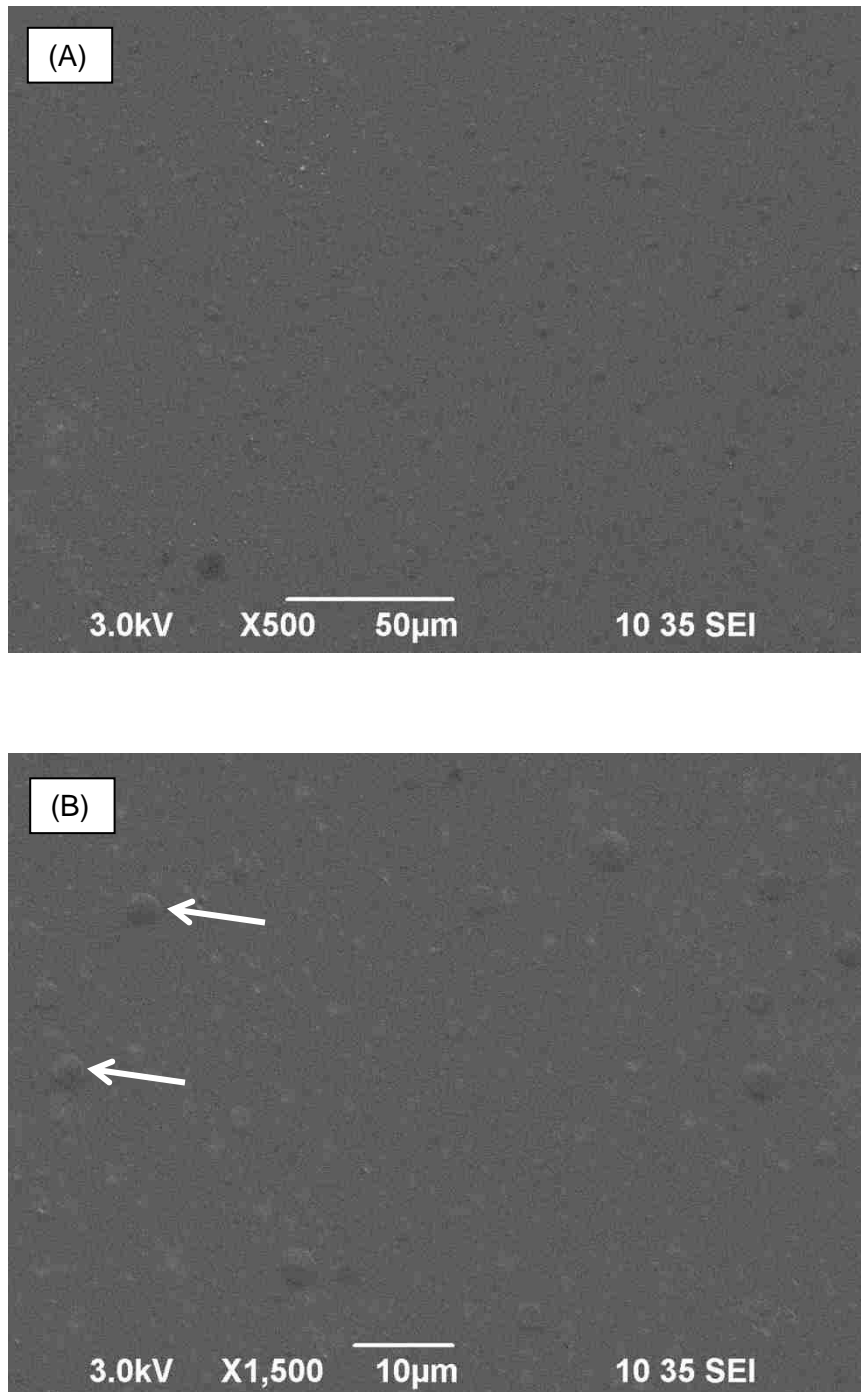


FIGURE 35. Representative SEM micrographs of 90 s etched ceramic with UR application (A) at $\times 500$ magnification and (B) at $\times 1500$ magnification. White arrows indicate bubbles

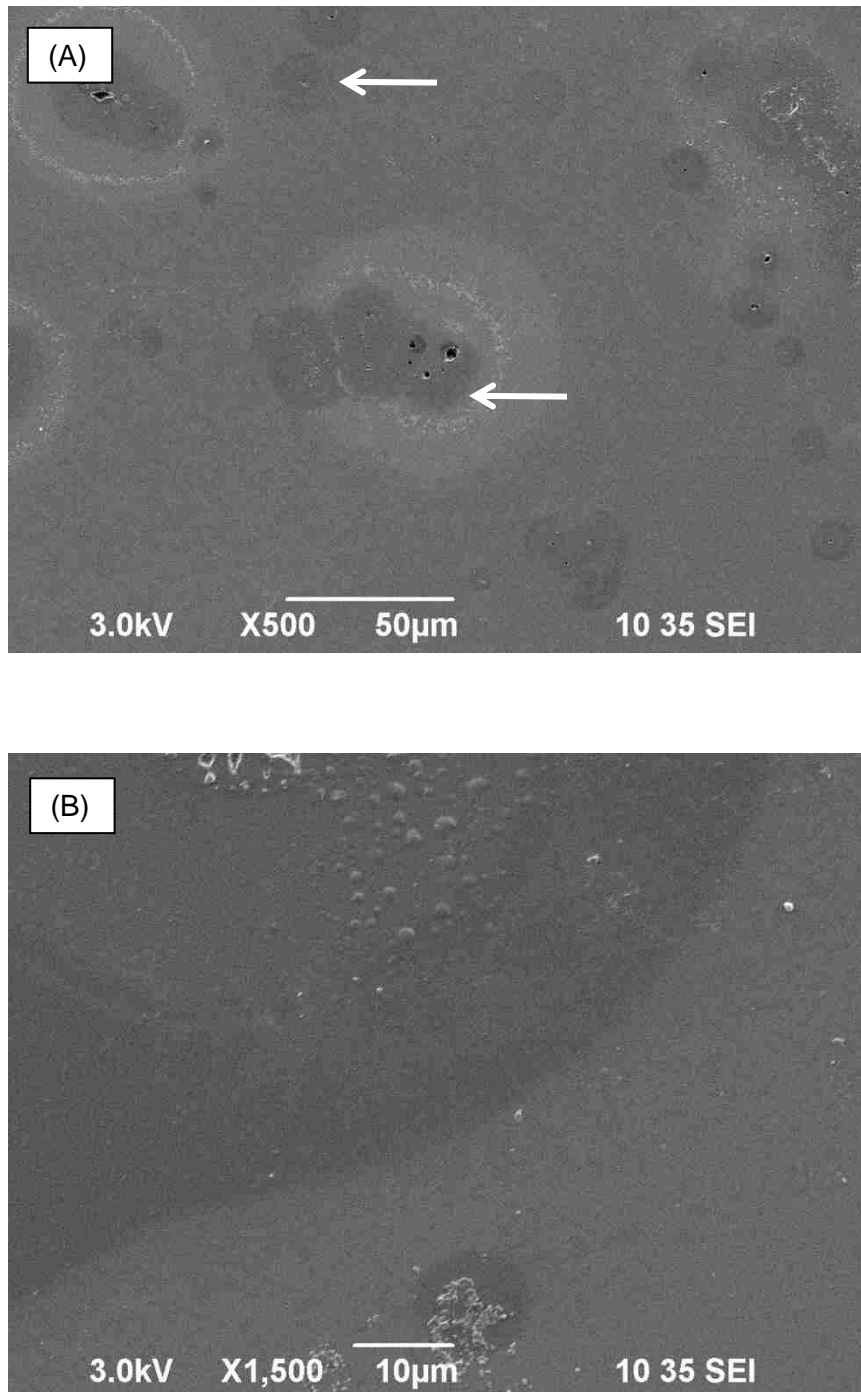


FIGURE 36. Representative SEM micrographs of 120 s etched ceramic with UR application (A) at $\times 500$ magnification, white arrows presents bubbles and (B) at $\times 1500$ magnification.

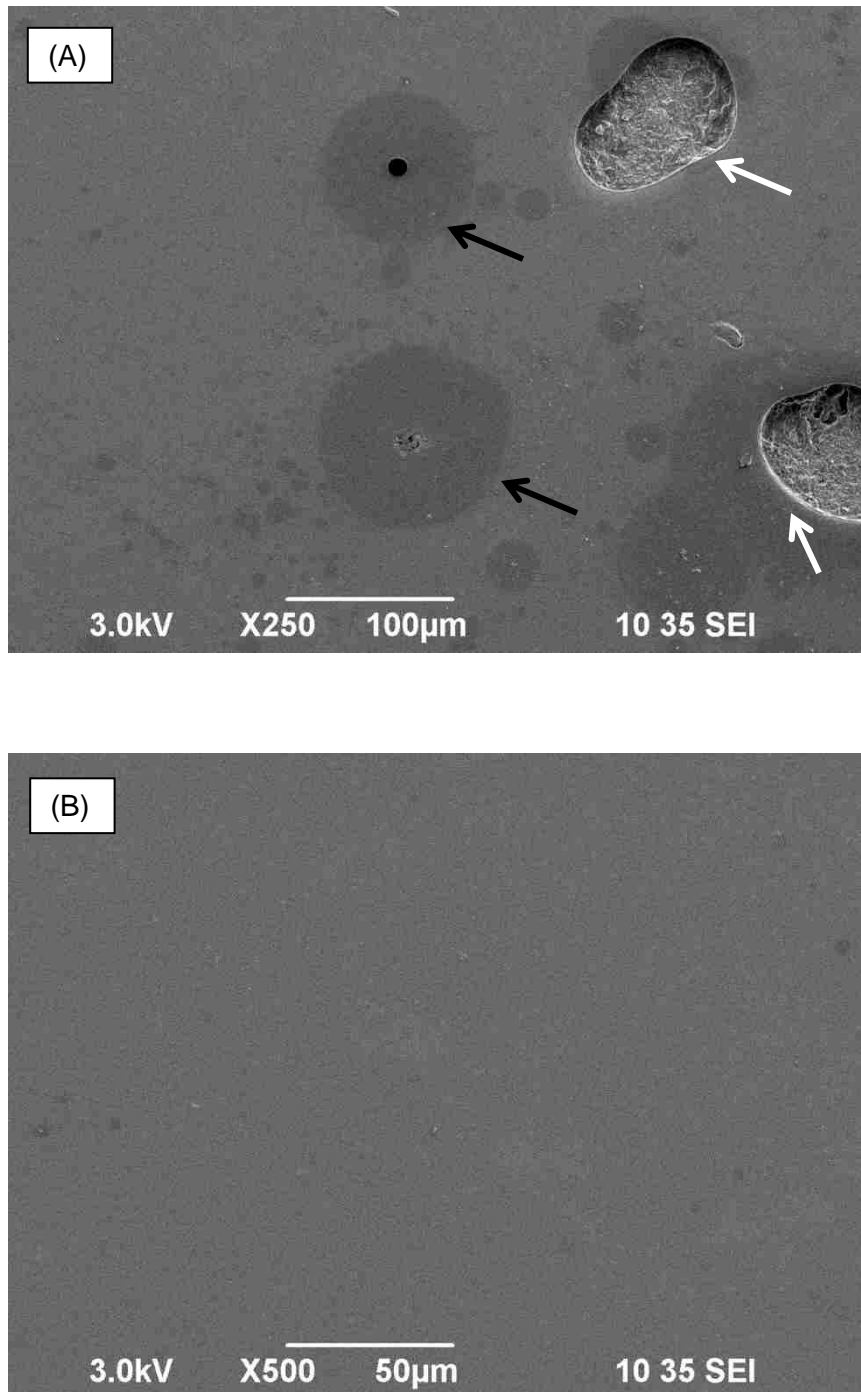


FIGURE 37. Representative SEM micrographs of re-etched ceramic with UR application (A) at $\times 250$ magnification and (B) at $\times 500$ magnification. White arrows indicate defect areas and black arrows shows bubbles.

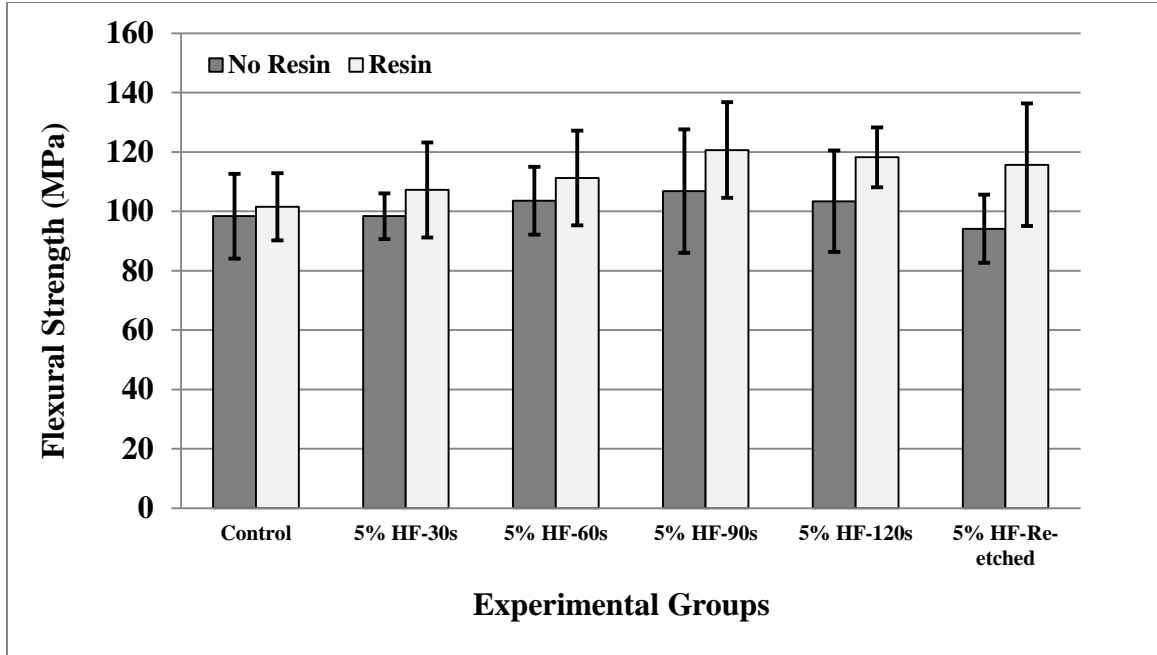


FIGURE 38. Flexural strength means and respective \pm SD of IPS ZirPress specimens

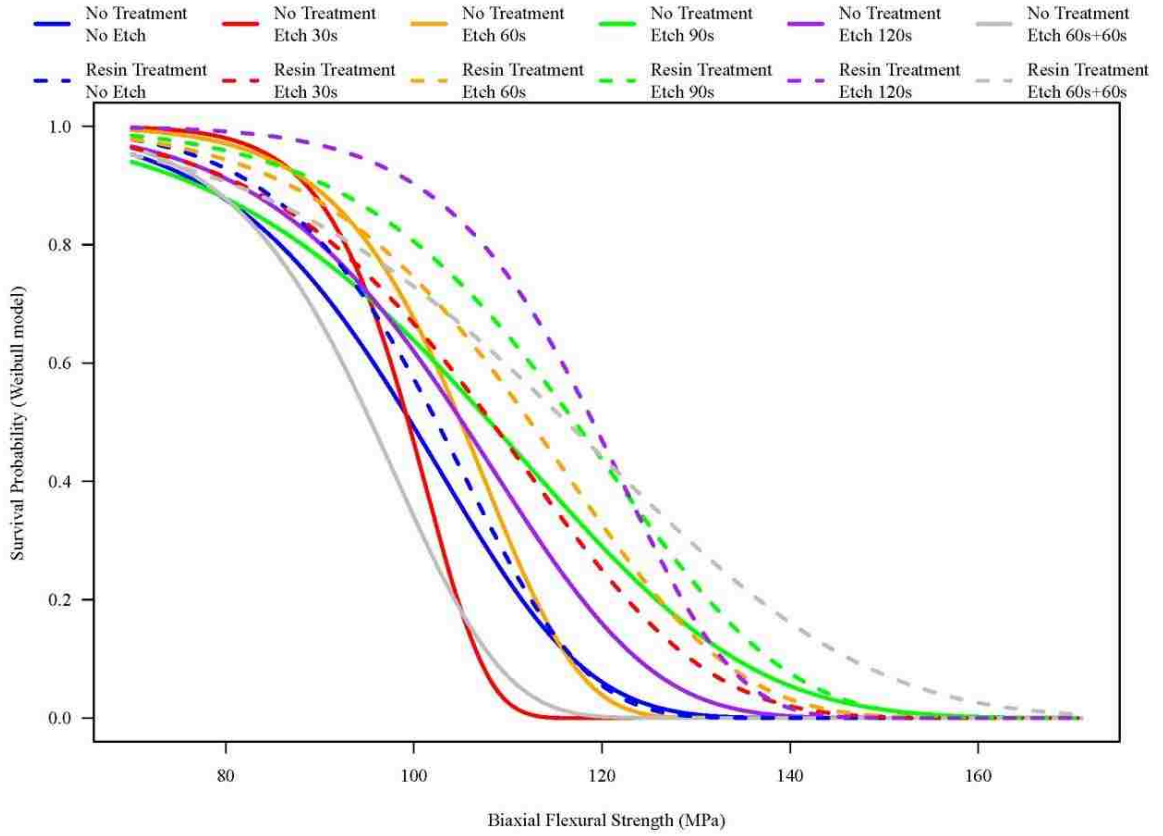


FIGURE 39. Survival probability plotted on Weibull model of experimental groups.

DISCUSSION

BIAXIAL FLEXURAL STRENGTH

Different sorts of flexural strength test (i.e., three- and four-point bending tests) have been employed to predict the performance of brittle materials such as dental ceramics. Essentially, the principle stress of these tests is tensile stress at the lower surface of the specimen that tends to cause cracks to originate from surface flaws and their propagation until a catastrophic failure occurs. The three-point bending test has been the standard test for dental ceramics since it is based on an uncomplicated test design test and the preparation of specimen in terms of shape and dimensions is relatively simple. More importantly, the most sensitive problem of this test is the presence of flaws along the surface edges.^{44,45} On the other hand, the biaxial flexural test has been considered more reliable than the uniaxial flexural test mostly due to the maximum tensile stresses occur in the central loading area, which eliminates the edge failure and generate less variation for the determination of material strength.^{44,45} Additionally, the biaxial flexural testing method reproduces the clinical mode of failure of all-ceramic restorations, i.e., failure from the extension of pre-existing flaws on the internal surface of restorations under tensile stress.^{17,19} The different designs of biaxial flexural strength tests include ball-on-ring, ring-on-ring and piston-on-three-ball. In our study we used the piston-on-three-ball configuration since it is known that the point contacts between the three balls and the disk-shaped specimen avoid undesirable stress when not perfectly flat specimens are used. Moreover, the diameter of the three balls oriented (10 mm) is smaller than the

disc specimen diameter (15 ± 1 mm); therefore, edge fracture can be prevented from direct loading, and also simulating pure bending.⁴⁶

EFFECT OF HF ACID SURFACE CONDITIONING ON CERAMIC FLEXURAL STRENGTH

This topic is still controversial; some studies^{3, 7, 29} indicated that HF acid etching significantly decreased the biaxial flexural strength of glass-based ceramics. On the other hand, Yen et al.⁴ reported the alteration of porcelain surfaces by HF acid etching at different etching regimens did not negatively impact the flexural strength of a feldspathic and a castable glass-ceramics. Similarly, Thompson et al.³⁶ found that the use of NH_4HF_2 had no significant difference on the biaxial flexural strength between non-etched and etched specimens a castable glass-ceramic. The present study corroborates with these findings. We found a significant effect of etching time ($p=0.0290$) on biaxial flexural strength for the ceramic tested. The etching time of 90 s had a significantly higher flexural strength (106.8 ± 21.7 MPa) than the control group (98.4 ± 14.9 MPa) ($p=0.0392$). Within this study conditions, surface morphology changes by acid etching and time of etch did not have a deleterious effect on the flexural strength of a fluorapatite ceramic.

One possible explanation of this finding could be the modification of surface flaws of IPS e.max ZirPress after HF acid treatment. Dental ceramics are brittle materials and the mechanical properties are associated with the variation in size and shape of initial flaws created during ceramic processing. Alterations in size and shape of initial surface flaws by HF acid etching have been associated with an increase in flexural strength most

probably due to a decrease in surface flaws size (e.g., reduce the size and the depth of surface flaws especially the small and sharp edges or tips of flaws and also round off the bottom of flaws).³⁶ Afterward, the smaller and smoother surface flaws would occur after HF acid treatment which could reduce the stress concentration at surface flaws that would enhance the flexural strength of IPS e.max ZirPress. However, when the etching time was increased to 120 s (G5) and re-etched (G6) groups, the flexural strength reduced to 103.4 ± 17.9 MPa and 94.1 ± 11.9 MPa, respectively. These findings could be explained that when the etching time was increase beyond a certain point; which in this study we observed above 90 s, the HF acid treatment would create smaller and deeper flaws at the base of the initial flaws. The stress concentration would be increase again then the flexural strength would be reduced.

THE EFFECT OF UNFILLED RESIN APPLICATION ON FLEXURAL STRENGTH

The results of current study obtained the biaxial flexural strength of all UR-treated groups were significantly higher than no resin treated groups ($p < 0.0001$). There may be several explanations of this finding. The mechanisms of resin strengthening etched ceramic have been proposed by many authors (e.g., crack closure by stress contraction; crack healed by cement and the recent one is hybrid ceramic composite layer).^{7, 17-19} Uhlmann et al.¹⁷ recommended the theory of the filling in or partial healing of surface flaws by decreasing the crack length, blunting the crack tip, crack contraction or their combination. Marquis et al.¹⁷ also suggested similar concept for crack shortening which surface flaws would be partially or totally filled with resin. A recent study by Addison et al.^{17, 18} proposed the hybrid ceramic composite layer theory, thereby the combination of

Poisson constraint and a resin inter-penetrated layer characteristic have the effect to the elastic modulus of that resin that may be strengthening the ceramic. They reported the ceramic surface roughness that was created by HF application or alumina particle abrasion could be penetrated by the filled resin, resulting in higher flexural strength than as fired ceramic specimens.

WEIBULL STATISTICS

A significant discrepancy in fracture stress among ceramic samples may occur due to the inherent distribution of flaws within materials, and thus the mean flexural strength may not be the true value. Alternatively, the so-called Weibull statistical method is used to describe this situation at any given load, a fraction of test specimens will survive.⁴⁷ The Weibull modulus is a material specific parameter similar but inversely related to standard deviation in normal distribution and is employed to describe the flaws distribution and data scattering. The large value of Weibull modulus ($m \geq 20$) certifies fewer fatal flaws, smaller in the strength estimation and greater clinical reliability. On the other hand, materials with initial flaws clustered unevenly present widely distribution of data, so the Weibull modulus in this group is low. The Weibull modulus values of dental ceramics are usually range from 5 to 15.^{26, 40, 48, 49} The current investigation obtained the Weibull moduli in almost experimental groups within this range except group 2 (30 s etching time) had the Weibull modulus 16.3. The explanation for this group may be from the fewer surface flaws from specimen preparation procedure. Another Weibull parameter in this study is Weibull characteristic strength (δn_0), which is the strength at the failure probability of 63.21%. The high value of δn_0 represents high strength of

material.^{48, 49} The current study revealed group of 90 s HF acid etching time showed the highest $\delta n0$ among non-treated groups. Moreover, all of UR treated groups presented the higher $\delta n0$ than non-treated group at the same etching time periods. Thus, the 90 s etching time can provide the good flexural strength specimens and also UR can improve the specimens strength.

Taken together, the obtained results led us to accept our first null hypothesis that HF acid etching time would not decrease the biaxial flexural strength of the glass-based veneering ceramic and to reject the null hypothesis that the biaxial flexural strength of etched glass-based veneering ceramic would not be restored by the UR treatment since our study found the flexural strength of IPS e.max ZirPress increased although the HF acid etching time increase until the certain point of HF acid etching time (90 s) Furthermore, we realized the resin strengthening mechanism after treatment the etched ceramic surfaces with the silane and UR , the flexural strength of all experimental groups had higher flexural strength.

CONCLUSIONS

Within the limitations of this *in vitro* study, the following conclusions were drawn:

1. HF acid etching time did not have the deleterious effect on the biaxial flexural strength of the IPS e.max ZirPress.
2. The recommendation etching time for IPS e.max ZirPress with 5% HF acid is 90 s in the term of mechanical properties and surface morphology.
3. The biaxial flexural strength of IPS e.max ZirPress could be enhanced by unfilled resin treatment.
4. The unfilled resin treatment before cement coating is recommended for IPS e.max ZirPress.

REFERENCES

1. Guess PC, Schultheis S, Bonfante EA, et al. All-ceramic systems: laboratory and clinical performance. *Dent Clin North Am* 2011;55(2):333-52, ix.
2. Griggs JA. Recent advances in materials for all ceramic restorations. *Dent Clin North Am* 2007;51:713-27.
3. Hooshmand T, Parvizi S, Keshvad A. Effect of surface acid etching on the biaxial flexural strength of two hot pressed glassceramics. *J Prosthodont* 2008;17:415-19.
4. Yen T-W, Blachman RB, Baez RJ. Effect of acid etching on the flexural strength of a feldspathic porcelain and a castable glass ceramic. *J Prosthet Dent* 1993;70(3):224-33.
5. Chaiyabutr Y, McGovan S, Phillips KM, Kois JC, Giordano RA. The effect of hydrofluoric acid surface treatment and bond strength of a zirconia veneering ceramic. *J Prosthet Dent* 2008;100(3):194-202.
6. Barghi N, Fischer DE, Vatani L. Effect of porcelain leucite content, types of etchants, and etching time on porcelain-composite bond. *J Esthet Restor Dent* 2006;18(1):47-53.
7. Addison O, Marquis PM, Fleming GJP. The impact of hydrofluoric acid surface treatments on the performance of a porcelain laminate restorative material. *Dent Mater* 2007;23:461-68.

8. Bottino MC, Ozcan M, Coelho PG, Bressiani JC, Bressini AHA. Micro-morphological changes prior to adhesive bonding: high alumina and glassy-matrix ceramics. *Braz Oral Res* 2008;22(2):158-63.
9. Naves L, Soares C, Moraes R, et al. Surface/interface morphology and bond strength to glass ceramic etched for different periods. *Oper Dent* 2010;35(4):420-27.
10. Oh W, Shen C, Alegre B, Anusavice K. Wetting characteristic of ceramic to water and adhesive resin. *J Prosthet Dent* 2002;88(6):616-21.
11. Ayad MF, Farmy NZ, Rosenstiel SF. Effect of surface treatment on roughness and bond strength of a heat pressed ceramic. *J Prosthet Dent* 2008;99(2):123-30.
12. Tylka DF, Stewart GP. Comparison of acidulated phosphate fluoride gel and hydrofluoric acid etchants for porcelain-composite repair. *J Prosthet Dent* 1994;72(2):121-27.
13. Canay S, Hersek N, Ertan A. Effect of different acid treatments on a porcelain surface. *J Oral Rehabil* 2001;28:95-101.
14. Kato H, Matsumara H, Atsuta M. Effect of etching and sandblasting on bond strength to sintered porcelain of unfilled resin. *J Oral Rehabil* 2000;27:103-10.
15. Roulet J, KJM S, J L. Effect of treatment storage conditions on ceramic/composite bond strength. *J Dent Res* 1995;74(1):381-87.
16. Guler AU, Yilmaz F, Yenisey M, Guler E, Ural C. Effect of acid etching time and self etching adhesive on the shear bond strength of composite rein to porcelain J *Adhes Dent* 2006;8(1):21-25.

17. Addison O, Marquis PM, Fleming GJ. Resin elasticity and the strengthening of all-ceramic restorations. *J Dent Res* 2007;86(6):519-23.
18. Addison O, Marquis PM, Fleming GJ. Resin strengthening of dental ceramics- the impact of surface texture and silane. *J Dent* 2007;35(5):416-24.
19. Addison O, Marquis PM, Fleming GJ. Quantifying the strength of a resin-coated dental ceramic. *J Dent Res* 2008;87(6):542-7.
20. Fleming GJ, Hooi P, Addison O. The influence of resin flexural modulus on the magnitude of ceramic strengthening. *Dent Mater* 2012.
21. Kelly JR, Benetti P. Ceramic materials in dentistry: historical evolution and current practice. *Aust Dent J* 2011;56 Suppl 1:84-96.
22. Denry I, Hollaway JA. Ceramics for Dental Applications: A Review. *Materials* 2010;3:351-68.
23. Conrad HJ, Seong WJ, Pesun IJ. Current ceramic materials and systems with clinical recommendations: a systematic review. *J Prosthet Dent* 2007;98(5):389-404.
24. Zarone F, Russo S, Sorrentino R. From porcelain-fused-to-metal to zirconia: clinical and experimental considerations. *Dent Mater* 2011;27(1):83-96.
25. Bottino MA, Salazar-Marcho SM, Leite FP, Vasquez VC, Valandro LF. Flexural strength of glass-infiltrated zirconia/alumina-based ceramics and feldspathic veneering porcelains. *J Prosthodont* 2009;18(5):417-20.
26. Salazar Marcho SM, de Melo RM, Macedo LG, Valandro LF, Bottino MA. Strength of a feldspar ceramic according to the thickness and polymerization mode of the resin cement coating. *Dent Mater* 2011;30(3):323-9.

27. Cattell MJ, Knowles JC, Clarke RL, Lynch E. The biaxial flexural strength of two pressable ceramic systems. *J Dent* 1999;27:183-96.
28. Albakry M, Guazzato M, Swain MV. Biaxial flexural strength, elastic moduli, and x-ray diffraction characterization of three pressable all-ceramic materials. *J Prosthet Dent* 2003;89(4):374-80.
29. Zogheib LV, Bona AD, Kimpara ET, McCabe JF. Effect of hydrofluoric acid etching duration on the roughness and flexural strength of a lithium disilicate-based glass ceramic. *Braz Dent J* 2011;22(1):45-50.
30. Ritter RG. Multifunctional uses of a novel ceramic-lithium disilicate. *J Esthet Restor Dent* 2010;22(5):332-41.
31. Ivoclar-Vivadent IPS e.max Zirpress Scientific Documentation. n.d.:World Wide Web Page:
http://communityconnectioncenter.com/.../IPSemax/zirpress_doc.pdf.
"http://communityconnectioncenter.com/DYNOTECH/ProductInfo/IPSemax/zirpress_doc.pdf".
32. Ivoclar-Vivadent emax ZirPress. n.d.:World Wide Web Page:
www.ivoclarvivadent.us/zoolu-website/media/.../IPS+e-max+ZirPress.
"www.ivoclarvivadent.us/zoolu-website/media/.../IPS+e-max+ZirPress".
33. Junpoom P, Kukiattrakoon B, Hengtrakool C. Flexural strength of fluorapatite-leucite and fluorapatite porcelains exposed to erosive agents in cyclic immersion. *J Appl Oral Sci* 2011;19(2):95-9.

34. Choi JE, Waddell JN, Torr B, Swain MV. Pressed ceramics onto zirconia. Part 1: Comparison of crystalline phases present, adhesion to a zirconia system and flexural strength. *Dent Mater* 2011;27(12):1204-12.
35. Torres SM, Borges GA, Spohr AM, et al. The effect of surface treatments on the micro-shear bond strength of a resin luting agent and four all-ceramic systems. *Oper Dent* 2009;34(4):399-407.
36. Thompson J, Anusavice K. Effect of surface etching on the flexural strength and fracture toughness of Dicor disks containing controlled flaws. *J Dent Res* 1994;73(2):505-10.
37. Chen JH, H. M, M. A. effect of different etching periods on the bond strength of a composite resin to a machinable porcelain. *J Dent* 1998;26(1):53-58.
38. Alex G. Preparing porcelain surfaces for optimal bonding. *Compend Contin Educ Dent* 2008;29(6):324-35; quiz 36.
39. Wagner WC, Chu TM. Biaxial flexural strength and indentation fracture toughness of three new dental core ceramics. *J Prosthet Dent* 1996;76(2):140-44.
40. Cattell MJ, Palumbo RP, Knowles JC, Clarke RL, Samarawickrama DYD. The effect of veneering and heat treatment on the flexural strength of Empress 2 Ceramics. *J Dent* 2002;30:161-69.
41. Fischer J, Stawarczyk B, Hammerle CHF. Flexural strength of veneering ceramics of zirconia. *J Dent* 2008;36:316-21.
42. Itinoche KM, Ozcan M, Bottino MA, Oyafuso D. Effect of mechanical cycling on the flexural strength of densely sintered ceramics. *Dent Mater* 2006;22(11):1029-34.

43. Addison O, Fleming GJP. The influence of cement lute, thermocycling and surface preparation on the strength of porcelain laminate veneering material. *Dent Mater* 2004;20:286-92.
44. Al-Makramani BM, Razak AA, Abu-Hassan MI. Biaxial flexural strength of Turkom-Cera core compared to two other all-ceramic systems. *J Appl Oral Sci* 2010;18(6):607-12.
45. Lin WS, Ercoli C, Feng C, Morton D. The Effect of Core Material, Veneering Porcelain, and Fabrication Technique on the Biaxial Flexural Strength and Weibull Analysis of Selected Dental Ceramics. *J Prosthodont* 2012.
46. Chen YM, Smales RJ, Yip KH, Sung WJ. Translucency and biaxial flexural strength of four ceramic core materials. *Dent Mater* 2008;24(11):1506-11.
47. Burrow MF, Thomas D, Swain MV, Tyas MJ. Analysis of tensile bond strengths using Weibull statistics. *Biomaterials* 2004;25(20):5031-5.
48. Thompson GA. Determining the slow crack growth parameter and Weibull two-parameter estimates of bilaminate disks by constant displacement-rate flexural testing. *Dent Mater* 2004;20(1):51-62.
49. Bona AD, Anusavice KJ, DeHoff PH. Weibull analysis and flexural strength of hot-pressed core and veneered ceramic structures. *Dent Mater* 2003;19(7):662-9.

ABSTRACT

EFFECT OF HYDROFLUORIC ACID ETCHING FOLLOWED BY UNFILLED
RESIN APPLICATION ON THE BIAXIAL FLEXURAL STRENGTH OF
A GLASS-BASED CERAMIC

By

Sumana Posritong

Indiana University School of Dentistry

Indianapolis, Indiana

Background: Numerous studies have reported the use of hydrofluoric (HF) acid as one of the most effective methods for the achievement of a durable bond between glass-based ceramics and resin cements. Nevertheless, there is little information available regarding the potential deleterious effect on the ceramic mechanical strength. **Objectives:** (1) to investigate the effect of HF acid etching regimens on the biaxial flexural strength of a low-fusing nanofluorapatite glass-ceramic (IPS e.max ZirPress, Ivoclar Vivadent), (2) to

study the ability of an unfilled resin (UR) to restore the initial (i.e., before etching) mechanical strength, and (3) to evaluate the effect of HF acid etching on the ceramic surface morphology before and after UR treatment via scanning electron microscopy (SEM). **Methods:** One hundred and forty-four disc-shaped (15 ± 1 mm in diameter and 0.8 ± 0.1 mm in thickness) IPS e.max ZirPress specimens were allocated into 12 groups, as follows: G1-control (no etching), G2-30 s, G3-60 s, G4-90 s, G5-120 s, G6- 60 + 60 s. Meanwhile, groups (G7- G12) were treated in the same fashion as G1-G6, but followed by silane and UR applications. Surface morphology evaluation of non-etched and etched IPS e.max ZirPress (G1-G12) was carried out by scanning electron microscopy (SEM). The flexural strength was determined by biaxial testing as described in ISO 6872. Statistics were performed using two-way ANOVA and the Sidak multiple comparisons ($\alpha = 0.05$). In addition, the Weibull statistics were estimated. **Results:** A significant effect of etching time ($p=0.0290$) on biaxial flexural strength was observed. Indeed, G4 led to a significantly ($p=0.0392$) higher flexural strength than G1. Correspondingly, G10 revealed a considerably higher flexural strength than G7 ($p=0.0392$). Furthermore, biaxial flexural strength was significantly higher for G7 – G12 than for G1 – G6 ($p<0.0001$). For G1 – G6, G4 showed the highest Weibull characteristic strength while the lowest Weibull characteristic strength was seen in G6. In G7 – G12, the highest Weibull characteristic strength was presented in G10 whereas G7 had the lowest. Finally, the SEM data revealed that the HF acid etching affected the surface of IPS e.max ZirPress by generating pores and irregularities and more importantly that the UR was able to penetrate into the ceramic microstructure. **Conclusion:** Within the limitations of this study, HF acid etching time did not show a damaging effect on the biaxial flexural

strength of the IPS e.max ZirPress ceramic. Moreover, the ceramic biaxial flexural strength could be enhanced after UR treatment.

CURRICULUM VITAE

Sumana Posritong

October 1974	Born in Nakorn Ratchasima, Thailand
May 1991 - March 1997	Doctor of Dental Surgery (DDS) Faculty of Dentistry, Khon Kaen University, Khon Kaen, Thailand
April 1997 - April 2000	Dentist Banbung Hospital, Chonburi, Thailand
May 2000 - April 2003	Dental General Practice Residency Institute of Dentistry Nonthaburi, Thailand
May 2003 - May 2009	Dentist and Instructor Institute of Dentistry Nonthaburi, Thailand
July 2009 – July 2012	M.S.D. Program (Prosthodontics) Indiana University School of Dentistry, Indianapolis, Indiana, USA

Professional Organizations

The Thai Dental Council (Thailand)

The Dental Association of Thailand

The Royal College of Dental Surgeons of Thailand

The John F. Johnston Society

The American College of Prosthodontics